Unilateral vestibular neurectomy induces a remodeling of somatosensory cortical maps

Justine Facchini, Guillaume Rastoldo, Christian Xerri, David Péricat, Abdessadek El Ahmadi, Brahim Tighilet, Yoh'i Zennou-Azogui

Progress in Neurobiology

Unilateral vestibular neurectomy induces a remodeling of somatosensory cortical maps

--Manuscript Draft--

Manuscript Number:	PRONEU-D-20-00395R3
Article Type:	Original Research Article
Keywords:	Vestibular Compensation; Cortical plasticity; Somatosensory; Tactile; Multisensory integration; Postural adjustments
Corresponding Author:	Justine Facchini Aix-Marseille Universite Marseille, FRANCE
First Author:	Justine Facchini, PhD Student
Order of Authors:	Justine Facchini, PhD Student
	Guillaume Rastoldo, PhD
	Christian Xerri, PhD
	David Péricat, Engineer
	Abdessadek El Ahmadi, PhD
	Brahim Tighilet, PhD
	Yoh'i Zennou-Azogui, PhD
Abstract:	Unilateral vestibular neurectomy (UVN) induces a postural syndrome whose compensation over time is underpinned by multimodal sensory substitution processes. However, at a chronic stage of compensation, UVN rats exhibit an enduring postural asymmetry expressed by an increase in the body weight on the ipsilesional paws. Given the anatomo-functional links between the vestibular nuclei and the primary somatosensory cortex (S1), we explored the interplay of vestibular and somatosensory cortical inputs following acute and chronic UVN. We determined whether the enduring imbalance in tactilo-plantar inputs impacts response properties of S1 cortical neurons and organizational features of somatotopic maps. We performed electrophysiological mapping of the hindpaw cutaneous representations in S1, immediately and 1 month after UVN. In parallel, we assessed the posturo-locomotor imbalance during the compensation process. UVN immediately induces an expansion of the cortical neuron cutaneous receptive fields (RFs) leading to a partial dedifferentiation of somatotopic maps. This effect was demonstrated for the ventral skin surface representations and was greater on the contralesional hindpaw for which the neuronal threshold to skin pressure strongly decreased. The RF enlargement was amplified for the representation of the ipsilesional hindpaw in relation to persistent postural asymmetries, but was transitory for the contralesional one. Our study shows, for the first time, that vestibular inputs exert a modulatory influence on S1 neuron's cutaneous responses. The lesion-induced cortical malleability highlights the influence of vestibular inputs on tactile processing related to postural control.
Suggested Reviewers:	Marie-Hélène Canu, PhD Professor, Unité de Recherche Pluridsciplinaire Sport, Santé, Société (URePSSS) marie-helene.canu@univ-lille1.fr Expert in hindpaw cortical mapping
	Fabrizio Strata, MD, PhD Assistant Professor, University of Parma: Universita degli Studi di Parma fabrizio.strata@unipr.it Expert in cortical plasticity
	Mathieu Beraneck, PhD CR, Université Paris Descartes: Universite de Paris Faculte de Sante mathieu.beraneck@parisdescartes.fr Expert in vestibular electrophysiology
	Andreas Zwergal, MD, PhD

	Professor, Ludwig-Maximilians-Universität München Adolf-Butenandt-Institut: Ludwig-Maximilians-Universitat Munchen Biomedizinisches Centrum Munchen Andreas.Zwergal@med.uni-muenchen.de Expert in vestibular compensation and vestibular cortex
Opposed Reviewers:	
Response to Reviewers:	

Unilateral vestibular neurectomy induces a remodeling of somatosensory cortical maps

Justine Facchini* & Guillaume Rastoldo*, Christian Xerri, David Péricat, Abdessadek El Ahmadi, Brahim Tighilet**, Yoh'i Zennou-Azogui**

Aix Marseille Université-CNRS, Laboratoire de Neurosciences Cognitives (LNC), UMR 7291, Marseille, France.

* J.F. and G.R. contributed equally to this study as co first-author.

** B.T. and Y.Z.A share senior authorship.

Correspondence to: Yoh'i Zennou-Azogui and Brahim Tighilet

Email: yohi.zennou-azogui@univ-amu.fr - brahim.tighilet@univ-amu.fr

Phone: +33413550861 - +33413550881

1. Introduction

Unilateral vestibular loss produces a well-known vestibular syndrome in humans and animals that includes posturo-locomotor, oculomotor and cognitive disorders whose expression gradually decreases over time (Curthoys and Halmagyi, 1995; Darlington and Smith, 2000; Lacour and Tighilet, 2010; Smith and Curthoys, 1989). To compensate for the loss of vestibular inputs, the central nervous system triggers multimodal sensory substitution and reweighting processes (Carriot et al., 2015; Jamali et al., 2014; Sadeghi et al., 2012, 2011, 2010; Xerri et al., 1983) that mainly take place within the vestibular nuclei, but also in other subcortical and cortical structures (Bense et al., 2004; Helmchen et al., 2009; Stiles and Smith, 2015; Zwergal et al., 2016). These processes that have remedial effects on the antigravity muscle asymmetries (Borel and Lacour, 1992; Lacour and Borel, 1993; Luccarini et al., 1992; Zennou-Azogui et al., 1993) are often accompanied by spontaneous individual postural strategies (Horak et al., 1990; Shupert et al., 1994) which need to be supplemented by rehabilitative procedures to more efficiently restore posturo-locomotor balance (Horak, 2009; Tjernström et al., 2016).

The typical temporal profile of posturo-locomotor deficits in rats subjected to unilateral vestibular neurectomy (UVN) is as follows: during the acute phase of the lesion (days 1 to 7) the animal's weight is consistently distributed on the contralesional paws to prevent disequilibrium and falling toward the lesion side. Then, the inverse pattern is observed and maintained from day 7 until at least one month postlesion, *i.e*. the body weight is shifted to the ipsilesional side (Marouane et al., 2020; Tighilet et al., 2017), and thus may reflect a long-term sensorimotor strategy in response to the posturo-locomotor instability induced by the vestibular lesion.

It has long been recognized that vestibular, visual, somatosensory and auditory inputs together contribute to the regulation of posturo-locomotor activities. Challenging the traditional view that multimodal integration takes place in associative cortical areas, recent studies have provided convincing evidence that primary sensory cortices are anatomically and functionally interconnected (for review see: Teichert and Bolz, 2018; Xerri and Zennou-Azogui, 2021). Anatomical tracing studies in rodents have demonstrated extensive direct corticocortical projections from the primary auditory cortex (A1) and the primary somatosensory cortex (S1) to the primary visual cortex (V1), from V1 to S1 and from A1 to S1 (Charbonneau et al., 2012; Henschke et al., 2015; Massé et al., 2017). The vestibular cortex differs from other sensory cortices in that vestibular signals are distributed in an extensive network of cortical regions (Brandt and Dieterich, 2019; Lopez, 2016;

Lopez and Blanke, 2011). An investigation in rats using both electrophysiological methods and fMRI mapping described the cortical projections of vestibular inputs to functionally diverse cortical regions that included S1 (Rancz et al., 2015). In addition, a more recent investigation revealed that the optogenetic stimulation of the medial vestibular nucleus neurons elicited bilateral fMRI activations in the sensorimotor cortices and their thalamic nuclei (Leong et al., 2019). Nevertheless, which region of S1 receives vestibular inputs and how the bimodal interplay occurs has not yet been investigated. We reasoned that the vestibulo-somatosensory convergence in S1 could occur in the cortical zones of the paw representations that would be congruent with the functional role of these inputs in the posturo-locomotor regulation. Accordingly, we evaluated the effects of a complete and irreversible vestibular loss on the response properties of S1 neurons in the hindpaw cutaneous representations. The *first aim* of our study is to gain insight into this multisensory cortical integration process by assessing whether and how acute unilateral vestibular deprivation may reveal a modulatory effect of the vestibular inputs on the cutaneous response of S1 neurons. To the best of our knowledge, this is the first investigation of the impact of a permanent vestibular deafferentation on the somatosensory cortical representations.

Furthermore, a wealth of studies on cortical plasticity have established that somatosensory cortical maps are not isomorphic representations of the body surfaces, but use-dependent, dynamically maintained representations which play a major role in the processing of behaviorally relevant sensory events underlying adaptive behavior (for review, see Xerri, 2008). Experience-dependent cortical map plasticity has been observed in all sensory systems during development and in mature brain, either after changes in sensory use (Jenkins et al., 1990; Xerri et al., 2005, 1999; Zennou-Azogui et al., 2016) or after an injury (somatosensory cortex: Merzenich et al., 1983; visual cortex: Hubel and Wiesel, 1964; auditory cortex: Robertson and Irvine, 1989; motor cortex: Sanes et al., 1990). Behaviorally relevant changes in somatosensory inputs leads to substantial alterations in the corresponding cortical representational area (Coq and Xerri, 1998; Polley et al., 2004; Rosselet et al., 2006; Xerri et al., 1996, 1994).

The rationale of this study lies at the junction of two lines of research hitherto investigated separately: the vestibular compensation phenomenon and the experience-driven plasticity of somatosensory cortical maps. Our research also stems from the available evidence showing that the body weight distribution has a profound remodeling effect on the fore- or hindpaw maps in S1 (Canu et al., 2007; Coq and Xerri, 1999; Zennou-Azogui et al., 2016). We focused on the representational areas of the hindpaws which are crucially involved in postural and locomotor stabilization as

indicated by the predominant weight distribution (~75%) on the hindlimbs in rats (Tighilet et al., 2017). The *second aim* of our study is to determine whether a long-lasting imbalance in the flow of peripheral tactilo-plantar inputs, induced by an enduring postural asymmetry following the UVN (Marouane et al., 2020; Tighilet et al., 2017), impacts the response properties of S1 cortical neurons and thereby affects the organizational features of the hindpaws cutaneous maps.

To achieve our aims, we performed cortical electrophysiological mapping of the hindpaws cutaneous representation in anesthetized rats, immediately and 1 month after the UVN. In parallel, we carried out a scoring procedure based on a qualitative behavioral assessment of the vestibular syndrome complemented with a quantitative automatized evaluation of the posturo-locomotor balance function during the course of the vestibular compensation.

2. Methods

2.1 Animals and experimental protocols

In this study, 33 male Long Evans rats weighing 300 ± 30 g were used. All experiments were performed in accordance with the National Institutes of Health's Guide for Care and Use of Laboratory Animals (NIH Publication no. 80-23), revised in 1996 for the UK Animals (Scientific Procedures) Act of 1986 and associated guidelines and the Policy on Ethics approved by the Society for Neuroscience in November 1989 and amended in November 1993 and under veterinary and National Ethical Committee supervision (French Agriculture Ministry Authorization: B13-055-25). The present study was approved by Neurosciences Ethics Committee N°71 of the French National Committee of animal experimentation. Every attempt was made to minimize both the number and the suffering of animals used in this experiment. Animals were housed under standard laboratory environmental conditions in groups of three in plexiglas cages (26.5 cm wide × 42.5 cm deep ×18 cm high). Food and water were provided *ad libitum*.

We performed electrophysiological cortical mapping of the hindpaw cutaneous representation in the S1 cortex in intact rats (CTRL, n=7). Mapping of the ipsilesional or contralesional hindpaws was initiated 1 hour after left UVN in two groups of animals ($1H_{ipsi}$ n=7; $1H_{cont}$ n=4) without waking up the animals, and 35 days after UVN in two other groups ($D35_{ipsi}$ n= 8; $D35_{cont}$ n=7). Among these postlesion groups, double cortical mapping was performed for the ipsilesional and contralesional hindpaws in the same rats at one hour (n=3) and 35 days (n=2) after UVN, starting with the

hemisphere either ipsilateral or contralateral to the lesion. We used the "resource equation" method developed by Mead (1988) to determine the total sample size. According to this method, if the error degrees of freedom (E) in an ANOVA is between about 10 and 20 or even more, then the experiment will be of an appropriate size (see also Festing and Altman 2002; Festing 2006). In a randomized design, E = (total number of animals) - (number of treatment combinations) and $10 < E < 20$. In our experimental design, $E = 33 – 5 = 28$.

Behavioral assessment of vestibular deficits and recovery was performed on days 1, 2, 3, 7, 10, 14, 21 and 30 after UVN in the animals mapped at the 35th day postlesion (n=15). In these rats, we measured the body weight distribution on the hindpaws at 2 time points: one day before and 35 days after UVN, prior to the electrophysiological recordings. Body weight distribution was also assessed in the CTRL rats, the day before the electrophysiological mapping of the S1 cortex (**Figure 1A**).

2.2 Surgical Procedures

2.2.1 Unilateral Vestibular Neurectomy

Animals were anesthetized with intraperitoneal injection of ketamine 1000 (25mg/kg, Virbac, France) and medetomidine (0.25mg/kg, Domitor® OrionPharma, Finland), and were subjected to a unilateral vestibular nerve section (UVN) on the left side. UVN was performed under visual control through a dissecting microscope. The vestibular nerve was completely sectioned after the Scarpa's ganglion, as close to the brainstem as possible. The body temperature was monitored using a rectal thermistor probe and was maintained between 37 and 38 °C with a feedback-controlled homeothermic blanket system (Harvard Apparatus Ltd., Kent, United Kingdom). UVN animals in which cortical mapping was to be performed 35 days after the lesion received an anti-inflammatory and analgesic treatment (Tolfédine, Vétoquinol; 4 mg/kg, i.m.). In addition, a solution of Ringer Lactate (Virbac; 10 ml/kg) was administered subcutaneously in order to alleviate the dehydration resulting from the inability of the animal to drink normally in the first days after the lesion. These animals were awakened by intraperitoneal injection of Antisedan® (Orion-Pharma; 1 mg/kg). The successful completion of the surgery was attested at the behavioral level by the presence of a characteristic vestibular syndrome (barrel rolling behavior, spontaneous nystagmus, etc.) and at the histological level by the observation under optical microscopy of the full section of the VIIIth cranial nerve between the Scarpa's ganglion and the brainstem (see Péricat et al., 2017, for details).

2.2.2 Preparation for cortical electrophysiological mapping

In $1H_{ipsi}$ and $1H_{cont}$ rats, cortical mapping was started about an hour after the lesion. Level of anesthesia with ketamine and medetomidine was monitored by testing the hindpaw reflex and was maintained by injecting half of the induction dose throughout the recording sessions. Local anesthetic (Xylocaïne, Xylovet®) was applied on the scalp and to the external auditory meatus to minimize pain generated by the ear-bars. The core temperature was continuously monitored and maintained between 37 and 38°C by a heating pad, as described above. The head of the animal was placed in a stereotaxic frame and a scalp incision was performed while attached muscles were retracted. Cerebrospinal fluid was drained through an opening in the dura covering the foramen magnum, after resection of posterior neck muscles, to prevent cerebral oedema. To expose the S1 cortex area to be mapped, a craniotomy (about 16 mm^2) was made with bregma as reference point (posterior: 1-5 mm; lateral: 2-6 mm) and the dura protecting the exposed cortex was resected. A thin layer of warm silicone fluid was applied to the cortical surface to prevent drying. During the mapping session, repeated injections of a cocktail of saline and glucose solution every 3 hours allowed the animal to be kept in a stable physiological condition. At the completion of the mapping session, the animal received a lethal dose of embutramide (T61, Med'Vet).

2.3 Cortical mapping procedure

Conventional multiunit recording and receptive field mapping techniques were used to reconstruct the hindpaw representation in layer IV of S1. The mapping procedure used in the present study has been described in detail in previous papers (Xerri et al., 2005, 1999). We used a high-resolution camera mounted on an operating microscope to obtain magnified images of the cortical area to be mapped and the contralateral ventral and dorsal surfaces of the hindpaw. An enlarged image of the exposed cortex was used to guide and record the location of electrode penetrations relative to the vasculature of the cortical surface. Recordings were performed with parylene-coated tungsten microelectrodes (about 1 MΩ at 1 kHz; WPI, UK) introduced perpendicular to the cortical surface and moved in cartesian coordinates using a three-dimensional micromanipulator driven by stepping motors (Märzhauser, FST; Germany). Sites of electrode penetration were identified relative to the vasculature of the cortical surface. For all rats, the interelectrode penetration distance ranged from 50 to 100 µm. The multi-unit signal was pre-amplified, filtered (bandwidth: 0.5–5 kHz), and displayed on an oscilloscope. This signal was also rectified and passed through a discriminator with an output

signal proportional to the part of the input signal which was higher than an adjustable threshold set just above the background noise. The output of the discriminator was then delivered to an audiomonitor. Using the recording artifact generated by the microelectrode contact with the cortex surface as a zero level, we advanced the electrode to a depth of about 650-700 microns to record responses from small clusters of neurons in layer IV (Waters et al., 1995; Welker et al., 1984). Under our recording conditions, the amplitude of the background noise usually ranged from 15 to 20 μV with a signal-to-noise ratio ranging from 4 to 6.

At each recording site, evoked cortical responses detected by large bursts of activity enabled us to classify neuronal responses as cutaneous or non-cutaneous. Cutaneous RFs were defined as the skin area where just-visible skin indentation or hair deflection elicited reliable changes in multi-unit activity. This stimulation was produced with a fine-tipped wooden stick and monitored using magnifying glasses (x4). Non-cutaneous responses were identified by taps and pressure on tendons, intrinsic muscle or joint manipulations while no cutaneous response was found. Cortical sites with only spontaneous discharges were classified as unresponsive. Ridges of the glabrous skin of the digits and the foot sole (*i.e.* palm) were used as reliable landmarks to delineate RFs. The cutaneous RF areas were measured offline using custom-written software (MATLAB®, Mathworks, Inc.).

The mechanical threshold of neuronal responses to skin stimulation recorded within the glabrous skin cortical sectors was determined using Von Frey monofilaments (Stoelting, Semmes-Weinstein aesthesiometer, Stoelting, Wood Dale, IL) that apply indenting stimuli at a relatively constant, predetermined force. The most commonly used filaments were 2.36 (bending force: 0.02 g; bending pressure: 4.39 g/mm^2): 2.44 (0.04 g; 4.93 g/mm^2); 2.83 (0.068 g; 5.37 g/mm^2), 3.22 (0.166 g; 9.15 g/mm^2), 3.61 (0.407 g; 16.36 g/mm^2), and 3.84 (0.692 g; 21.39 g/mm^2). We used a stimulus series of increasing and decreasing strengths to determine the mechanical threshold eliciting noticeable changes in neuronal discharge. The stimulation consisted in pressing a filament gently against the ventral skin, perpendicular to its surface and at the center of the RF, until the filament began to bend. This procedure was done 5 to 10 times for each filament. The mechanical threshold is conventionally used as a measure of neuronal response sensitivity.

After the recording session, we used Canvas software (ACD Systems) to make a cutaneous map of the hindpaw by drawing boundaries encompassing cortical sites whose RFs were restricted to a common hindpaw subdivision (*e.g.,* digit, palm, heel, etc.). When RFs were located on distinct and separate skin subdivisions, borders were drawn midway between adjacent recording sites. When a

single RF included different but adjoining skin subdivisions of the hindpaw, a boundary line was drawn that crossed cortical sites. Borders were drawn midway between responsive and unresponsive sites **(Figure 1B-C)**. When RFs were located on two or more hindpaw skin subdivisions, we pooled together cortical sites in specific map sectors referred to as "*mixed*" areas. Cortical sectors defined as "*paw*" included recording sites in which RFs included the whole ventral or dorsal paw surface.

2.4 Behavioral assessment of the vestibular syndrome

The vestibular syndrome was scored after UVN based on 10 behavioral components following a procedure previously described (Rastoldo et al., 2020): tail hanging reflex, landing reflex, rearing, grooming, displacement, head-tilt, barrel rolling, retropulsion, circling and bobbing. Each session lasted about 15 min and was videotaped for off-line analysis.

- Tail hanging reflex: animals were picked up from the ground at the base of the tail and body rotation around z gravitational axis was scored from 0 (*no rotation*) to 3 points (*several rotations of 360°*).
- Landing reflex: after animals were picked up from the ground at the base of the tail, we scored the first 3 landings from 0 to 3 points (*presence or absence of landing reflex on the 3 landings, respectively*).
- Rearing: the ability of the rat to rear was scored from 0 point (*rearing is observed*) to 1 point (*rearing is absent*).
- Grooming: the ability of the rat to groom was scored as follows: 0 point (*correct grooming of full body*), 1 point (*grooming of the face, belly and flanks, but not the base of the tail*), 2 points (*grooming limited to the face and belly*), 3 points (*grooming of the face*), 4 points (*inability of the animal to groom itself*).
- Displacement: quality of the rat locomotion was scored from 0 (*displacement with no visible deficit*) to 3 points (*several deficits in the displacement, e.g., path deviation, falls, etc.*).
- Head tilt was scored by estimating the angle between the jaw plane and the horizontal with 0 points (*absence of a head-tilt*) to 3 points (*for a 90° angle*).
- Barrel rolling about the horizontal body axis was scored as follows: 0 points (*absence of barrel rolling*), 1 point (*barrel rolling triggered by an acceleration in the vertical axis of the rat in our hand*), 2 points (*spontaneous barrel rolling*).
- Retropulsion characterizes backward movements and was scored from 0 (*absence of retropulsion*) to 1 point (*presence of retropulsion*).
- Circling about the vertical axis was scored from 0 (*absence of circling behavior*) to 1 point (*presence of circling behavior*).

- Bobbing is assimilated to cephalic nystagmus and was scored from 0 (*absence of bobbing*) to 1 point (*presence of bobbing*).

A mean score was calculated by adding the points obtained for the different quantified components. For each rat, a mean score was collected the day before the lesion as a reference value, and at days 1, 2, 3, 7, 10, 14, 21 and 30 postlesion.

2.5 Support surface

Static postural deficits and recovery were evaluated by measuring the support surface delimited by the four legs of the rat, after the tail hanging landing test. The support surface can be regarded as a good estimate of postural control because it reflects the rat's behavioral adaptation compensating for the static vestibulospinal deficits induced by the vestibular lesion. This test consisted in taking the animal by the tail and lifting it vertically over a height of about 50 cm (*lift duration 2 s; position holding at upper position: 1 s*). To quantify the support surface, rats were placed in a device with a graduated transparent floor that allowed them to be filmed from underneath. A scale drawn on the floor served to take measurements of the location of the four paws. When the animal landed on the ground, a picture was captured. The support surface was measured using a custom-written image analysis tool (MATLAB®, Mathworks, Inc.). At each testing session, twenty repeated measurements were taken, and an average value was calculated for each rat. Data were first acquired the day before the lesion, serving as a reference value, and then at days 1, 2, 3, 7, 10, 14, 21 and 30 postlesion. For each rat, data recorded after UVN were compared to the reference value obtained in the same animal.

2.6 Body weight distribution

The body weight distribution of the animals was quantified with a DWB1 device (BIOSEB; France). This device consists of a plexiglas cage (25x25 cm) in which the animal is placed for 5 min recordings while moving freely. The floor of this cage is covered with a plate equipped with 2000 force sensors. Sensors detect vertical pressure at a sample rate of 30 Hertz. They are connected to an electronic interface that converts the current flowing through it into a measure of weight, the whole being connected to a computer. The cage is closed by a lid on which a high definition camera connected to the computer through a USB cable is secured. We measured the weight distributed on the ipsi- and contralesional hindpaws before UVN and at 35 days postlesion (D35). In order to compensate for the weight variability of the rats, the weight distribution on the hindpaws was

expressed as a percentage of the animal body weight on the day of acquisition (before the lesion or D35 after UVN). In a previous work (Tighilet et al., 2017), we have shown that, before the lesion and 30 days after the lesion, rats spent about 50% of the time in bipedal stance and 50% in quadrupedal stance. Therefore, body weight distribution on the hindpaws was analyzed separately for these two postural patterns.

2.7 Experimental measurements

Cutaneous glabrous and hairy RFs were measured in mm^2 and normalized relative to the total (ventral + dorsal) cutaneous surface of the hindpaw measured on the digitized images. The mean relative size of all recorded RFs was computed for each experimental group. The different cutaneous sectors of the hindpaw map (*simple* and *mixed* ventral or dorsal skin hindpaw territories) were measured in mm^2 and normalized relative to the whole map area. These normalized values were averaged for each experimental group. The mechanical thresholds of neuronal responses to stimulation of hindpaw ventral skin (*i.e.*, of ventral and ventral&dorsal RFs) obtained using the Von Frey filaments were processed to calculate an average pressure threshold (g/ mm^2) for each group.

2.8 Statistics

Average percentage of the body mass applied on left and right hindpaw was calculated before UVN lesion (Pre-op) and at 35 days postlesion (D35) and compared (Left vs. Right hindpaw or Bipedal vs. Quadrupedal stance for the same animal) using a paired *t-test*. The statistical analyses of the support surface data were evaluated by ANOVA using Dunnett's *post-hoc* comparison test (GraphPad, Prism). Comparison of variances was performed using the Bartlett homogeneity of variance test.

As the RF sizes were not normally distributed, statistical analyses were carried out using non-parametric tests to make comparisons between all experimental groups. We first performed a Kruskal-Wallis H test to detect differences between the CTRL and the lesioned groups. Data in these lesioned groups have been treated using a design with two-level postlesion delay (1H and D35) and the two-level hindpaw side (ipsi- and contralesional) as crossed factors. Hence, we used a Scheirer-Ray-Hare test which is a multifactorial extension of the Kruskal-Wallis test (Scheirer et al., 1976) to reveal main effects of these two factors and their interaction. All these statistical analyses were supplemented with the *post-hoc* Dunn test. These analyses were also performed on absolute values of thresholds of

responses to cutaneous stimulation (pressure, g/mm^2) for between-group comparisons of neuronal sensitivity. Moreover, we investigated whether RF size was associated with neuronal sensitivity in each experimental group. ANCOVA was carried out with neuronal threshold as dependent variate and RF size as a covariate of the group factor. This analysis allows testing regression slope homogeneity across experimental groups by detecting the interaction between group levels and the covariate.

Statistical treatment of the normalized cortical areas was performed using ANOVA supplemented with multiple comparisons (contrast *post-hoc* test; JASP software, version 0.14.1). Repeated-measures ANOVA (1-between, 2-within) was used to compare ipsative data (*i.e.*, a set of responses that always sums to 100%; cf. Greer and Dunlap 1997) consisting of the proportions of cortical areas representing hindpaw skin sectors (ventral or/and dorsal) within the defined categories (*simple*, *mixed*) of the map regions. The between factor consisted in the 5 levels group, whereas the category and hindpaw skin sectors were considered as within factors.

Mean (± SEM) values are used throughout the manuscript. Median values (± IQR) are also shown in some figures.

3. Results

3.1 Vestibular deficits induced by UVN

A quantitative assessment of the vestibular syndrome allows a global evaluation of the vestibular compensation process. Immediately after the surgical unilateral vestibular neurectomy, rats displayed posturo-locomotor impairments characteristic of the vestibular syndrome. These deficits expressed by a 'vestibular score' based on 10 behavioral components were analyzed at different time points over the first four weeks following the vestibular lesion (**Figure 2A**). One day after the UVN, the mean vestibular score reached its maximum level (15.82 ± 0.71). Over the subsequent weeks, the behavioral deficits progressively diminished in two main phases. In the first phase, during the first 10 days postlesion, we observed a progressive and linear decrease of the vestibular score that reached a value of 9.25 ± 1.15 at D10. In the second phase, over the subsequent three weeks, the vestibular score reached a plateau. It is noticeable that the dispersion around the mean values gradually diminished during this period of time (D10 vs D30: $p < 0.0001$), illustrating stronger similarities in the behavioral patterns across animals. At this stage, several residual deficits were found, such as

head tilt, tail-hanging reflex and locomotion impairment, whereas the barrel rolling, retropulsion and circling behaviors were no longer observed. The UVN also resulted in an increase in the support surface delimited by the animal's four paws. This parameter is commonly used to describe postural stability and restoration of balance (Dutheil et al., 2016; Liberge et al., 2010; Marouane et al., 2020; Tighilet et al., 2019, 2018). Our present results show that in UVN rats, the support surface area was significantly increased throughout the first 3 days postlesion (D1 to D3: $p < 0.0001$) and gradually returned to pre-operative values from D7 to D30 (p: ns; **Figure 2B**).

Then, we quantified the percentage of weight distribution along the lateral body axis, between the left and right hindpaws (**Figure 2C**). Before the lesion, freely moving rats distributed their weight equally between the left and right hindpaws (41.78 ± 0.72 % vs 41.24 ± 1.22 %). These results are consistent with those previously described for the distribution of the body weight on the fore- and hindpaws (Marouane et al., 2020; Tighilet et al., 2017). At D35 after UVN, rats exhibited a significant increase of their weight on the left (ipsilesional) hindpaw (47.08 ± 1.55 %, $p < 0.001$). We also separately evaluated the difference in percentage of body weight applied on the ipsilesional (left) hindpaw between bipedal and quadrupedal stance. The results are qualitatively similar for bipedal and quadrupedal stances. However, a statistically significant increase in the weight applied to the ipsilesional hindpaw was found in bipedal stance at D35 after UVN (58.83 ± 2.01 %, $p < 0.001$) whereas the increase in the quadrupedal stance was not found to be significant (49.60 ± 0.93 %, $p = 0.0598$) **(Figure 2D).** Since the hindpaws are more frequently in contact with the ground than the forepaws, and in view of the present behavioral findings, our electrophysiological recordings targeted the cortical zone of S1 serving the hindpaw representation.

3.2 Remodeling of the hindpaw cutaneous representation following UVN

3.2.1 Changes in size and spatial distribution of cutaneous receptive fields

Each individual cortical map was reconstructed on the basis of about 60 recording sites per animal. We recorded a total number of 786 cutaneous RFs in 33 rats. We first asked whether the vestibular deafferentation immediately impacts the S1 neurons response properties. We found that the spatial extent of the cutaneous RFs was significantly altered (**Figure 3A, B).** A significant increase in the mean RF size was indeed recorded during the first hours postlesion (CTRL: 6.14 ± 0.32 %, 1H: 9.90 ± 0.48 %; $p < 0.001$**)**. A more detailed analysis revealed that these postlesion changes applied to both ipsilesional ($1H_{ipsi}$: 8,74 ± 0.48 %; $p < 0.0001$) and contralesional hindpaw RFs ($1H_{cont}$: 12.37 ±

1.02 %; $p < 0.00001$) (**Figure 3B**). Comparison between the ipsi- and contralesional RFs, however, showed a greater increase on the contralesional hindpaw ($p < 0.02$). To gain further insight into the cortical impact of the vestibular deafferentation, we distinguished the ventral from dorsal skin RFs for both the contra- and the ipsilesional S1 cortex (**Figure 3C, D**). Hence, the RFs located on both ventral and dorsal skin surfaces (13.93 %) were discarded from analysis. First, considering the ventral skin RFs, we found that, compared to the intact rats, ventral skin RFs increased on both the ipsilesional (CTRL: 5.77 ± 0.33 %, $1H_{ipsi}$: 8.55 ± 0.52 %; $p = 0.0001$) and contralesional ($1H_{cont}$: 11.97 ± 0.97 %; $p = 0.00001$) hindpaws. However, the ventral RF expansion was greater on the contralesional than the ipsilesional hindpaw ($p = 0.02$). Then, considering the dorsal skin RFs, the increase recorded during the first hours postlesion was not statistically significant (CTRL: 7.87 ± 0.97 %, $1H_{ipsi}$: 10.20 ± 1.04 %, $1H_{cont}$: 19.88 ± 9.01 %; $p = 0.66$ and $p = 0.68$ respectively). Overall, our data show that the main early effect of the UVN is a bilateral increase of the ventral skin RF size. However, this increase is more prominent on the contralesional hindpaw.

Compared to the CTRL map, 35 days after the lesion, we observed a substantial enlargement of the RFs located on the ipsilesional hindpaw (CTRL: 6.14 ± 0.32 %, $D35_{ipsi}$: 16.98 ± 0.88 %; $p < 0.00001$ **(Figure 3B)**. This increase was shown to be even greater than that recorded in the few hours after the lesion ($1H_{ipsi}$ *versus* $D35_{ipsi}$: $p < 0.001$). This ipsilesional expansion led to a striking difference with the contralesional hindpaw RFs ($p < 0.00001$) for which no difference with respect to control values was found ($D35_{cont}$: 7.62 ± 0.71 %; $p = 1$). At D35 postlesion, we also compared separately the ventral and dorsal skin RFs after discarding from analysis the RFs located on both the ventral and dorsal skin surfaces (17.09 %) **(Figure 3C, D)**. We reasoned that the postural imbalance increasing the body weight on the ventral surfaces of the ipsilateral hindpaw would selectively modify the ventral skin territories in the corresponding cortical map. Ventral skin RFs increased on the ipsilesional hindpaw as compared to CTRL (CTRL: 5.77 ± 0.33 %, $D35_{ipsi}$: 16.66 ± 0.91 %; $p < 0.00001$), and more prominently than during the first hours postlesion ($1H_{ipsi}$ *versus* $D35_{ipsi}$: $p < 0.00001$). By contrast, a return to a normal size was found for the ventral RFs on the contralesional hindpaw ($D35_{cont}$: 5.94 ± 0.54 %, CTRL *versus* $D35_{cont}$: $p = 1$), indicating a strong asymmetrical alteration between ventral RFs on ipsi- and contralesional hindpaws at D35 ($p < 0.00001$) (**Figure 3C**). The dorsal skin RFs increased on the ipsilesional hindpaw as compared to CTRL (CTRL: 7.87 ± 0.97 %, $D35_{ipsi}$: 19.37 ± 3.13 %; $p < 0.001$), but not on the contralesional hindpaw ($D35_{cont}$: 13.53 ± 2.30 %, CTRL *versus* $D35_{cont}$: $p = 1$). However, contrasting with the asymmetry of ventral RFs, dorsal RFs were not found to be significantly different between the two hindpaws ($D35_{ipsi}$ *versus* $D35_{cont}$: $p = 0.15$) (**Figure 3D)**.

We assessed the mechanical threshold of the neuronal responses reflecting the minimum sensitivity to pressure exerted at the center of their RFs. Interestingly, a lesion-induced asymmetry was found between the cortical areas representing the ipsi- and contralesional hindpaws, depending on the postlesion time. During the first hours postlesion, the neuronal sensitivity in the cortical area representing the contralesional hindpaw was greater than that of the ipsilesional one, as attested by smaller thresholds of response to the mechanical stimulation of ventral skin surfaces of the contralesional hindpaw ($1H_{contra}$: 7.55 ± 0.53 g/mm^2, $1H_{ipsi}$: 12.99 ± 1.59 g/mm^2; $p < 0.00001$). The reverse was observed at D35 ($D35_{contra}$: 13.75 ± 0.49 g/mm^2, $D35_{ipsi}$: 11.01 ± 0.43 g/mm^2; $p < 0.0001$) as the neuronal sensitivity within the area of the contralesional hindpaw strongly decreased ($p < 0.00001$) (**Figure 4A**). We searched for a possible correlation between the neuronal RF size and sensitivity. When data were log-log plotted, the trends within each experimental group presented negative linear relationships between threshold of response to skin pressure and RF size suggesting that the data follow a power law relationship under the form $y \propto x^{-\beta}$, between neuronal sensitivity (y) and RF size (x). (**Figure 4B**). Moreover, ANCOVA did not reveal statistically significant interaction between RF size and experimental group factor [$F(4, 532) = 1.86$; $p = 0.116$], indicating an acceptable hypothesis of identical slope coefficients for all the experimental groups [$\beta = -0.155$; $t(536) = -4.98$; $p < 0.001$]. Therefore, in all groups, we found that the larger the RF size, the greater the sensitivity (i.e., the smaller the response threshold to skin pressure). It is noteworthy that in the cortical area of the hindpaw opposite to the lesion side, a strong increase of neuronal sensitivity was recorded during the first hours postlesion, regardless the RF size [Δ intercept = - 0. 103, $t(536) = -3.03$; $p = 0.003$] (**Figure 4B**).

To ensure that postlesion alterations were not blurred by interindividual differences, we also performed mapping of both hemispheres in each postlesion group (1H n= 3, D35 n=2, see **Supplementary Figure 1**. This double mapping corroborates both the bilateral expansion of ventral RFs at 1H postlesion and only on the ventral ipsilesional hindpaw 35 days after the UVN, as well as the postlesion asymmetry in neuronal sensitivity. Therefore, in this respect, these animals can be seen as representative of their own experimental group. Such a conclusion cannot be drawn for the dorsal RFs, given the small size of the sample collected.

3.2.2 Organization of hindpaw somatosensory maps

The somatotopic organization of the hindpaw representation within the intact S1 cortex of rats displayed invariant organizational features despite inter-individual differences in representational details. The hindpaw cutaneous representation was consistently located medial and posterior to the forepaw map and in a medial-rostral location with respect to the tail and back representations. From rostral to caudal, the somatotopic organization was revealed by the progression of cortical sites from the toes, plantar pads of the sole to the heel. The cutaneous representation displayed a somatotopic order that clearly segregated individual digits and plantar pads, qualified as *simple* areas, that were ordered from the anterolateral to posteromedial cortical sector **(Figure 5A)**. Additionally, control animals showed *mixed* areas corresponding to neurons with RFs localized on 2 or more skin territories of the paw.

After the lesion, the overall map size was not affected either at one hour (CTRL: 0.93 ± 0.12 mm^2, $1H_{ipsi}$: 0.78 ± 0.08 mm^2, p: n.s.; $1H_{cont}$: 0.90 ± 0.19 mm^2, p: n.s.) or at 35 days postlesion ($D35_{ipsi}$: 0.86 ± 0.13 mm^2, p: n.s.; $D35_{cont}$: 0,82 ± 0.18 mm^2, p: n.s.) **(Figure 5B)** for both hindpaw representations. However, the postlesion increase in RF size, described above, led to changes in the proportion of each representational area (*simple* and *mixed*) of the somatotopic map, *i.e.* a fusion of previously segregated areas.

Immediately after the lesion, we observed a significant bilateral diminution of the proportion of *simple* areas (CTRL: 90.49 ± 2.31 %, $1H_{ipsi}$: 73.52 ± 3.64 %, $p < 0.0001$; $1H_{cont}$: 71.02 ± 5.03 %, $p < 0.0001$) related to an extension of *mixed* areas (CTRL: 9.51 ± 2.31 %; $1H_{ipsi}$: 26.49 ± 3.64 %, $p < 0.0001$; $1H_{cont}$: 28.98 ± 5.03 %, $p < 0.0001$) in both the ipsilesional and contralesional hindpaw maps **(Figure 5C)**. The expansion of the *mixed* areas reflects a partial dedifferentiation of the somatotopic maps. No differences between ipsi- and contralesional hindpaw maps were noticed (*simple* areas, p: n.s.; *mixed* areas, p: n.s.).

At 35 days postlesion, a drastic reduction of the relative extent of *simple* areas (CTRL: 90.49 ± 2.31 %; $D35_{ipsi}$: 36.22 ± 5.28 %, $p < 0.0001$) combined with an expansion of the *mixed* areas (CTRL: 9.51 ± 2.31%; $D35_{ipsi}$: 63.78 ± 5.28 %, $p < 0.0001$) was found in the map representing the ipsilesional hindpaw. By contrast, a differentiation between cortical sectors of the contralesional hindpaw map was observed, approaching that found in prelesional maps (*simple* areas: $D35_{cont}$, 65.35 ± 20.61 %, $p < 0.05$; *mixed* areas: $D35_{cont}$ 25.97 ± 12.42 %, p: n.s.) **(Figure 5C)**. The somatotopic dedifferentiation resulting from the ipsilesional hindpaw map changes is mostly attributed to the substantial shrinkage of the *simple* ventral areas (CTRL: 71.94 ± 4.19 %; $D35_{ipsi}$: 25.23 ± 5.48 %, $p < 0.0001$) and a prominent increase of the *mixed* ventral areas (CTRL: 7.80 ± 2.40 %; $D35_{ipsi}$: 40.57 ± 5.80 %, p <

0.001) **(Figure 5D)**. As for the contralesional hindpaw map, the data show no significant differences between control values and either ventral (*simple* areas: p: n.s.; *mixed* areas: p: n.s.) or dorsal (*simple* areas: p: n.s.; *mixed* areas: p: n.s.) skin areas **(Figure 5D, E)**.

4. Discussion

This study confirms previous findings on the time course of the postural strategy of rats subjected to a permanent unilateral loss of vestibular afferents, characterized by a support surface enlargement from day 1 to day 3 after the lesion and a predominant weight distribution on the ipsilesional hindlimb from day 7 that persisted at least until day 35. Based on electrophysiological recordings of small clusters of neurons in the primary somatosensory cortex, we demonstrate, for the first time, that the unilateral vestibular neurectomy (UVN) induces, over the first hours following the vestibular loss, a bilateral expansion of the cutaneous RF of the hindpaws. This expansion was conclusively demonstrated for the ventral skin surfaces and was greater on the contralesional hindpaw. Neurons within the cortical area representing this contralesional hindpaw displayed a greater sensitivity to skin mechanical stimulation. As a result of RF enlargement, a bilateral degradation of the spatial grain of representation of the cutaneous map of the hindpaws occurred. The overall surface area of the hindpaw cortical map was not modified immediately after UVN.

Thirty-five days after the lesion, the expansion of ventral cutaneous RFs on the ipsilesional hindpaw was even greater than early after the UVN, whereas the ventral RFs on the contralesional hindpaw returned to normal. This latter effect was accompanied with a strong decrease in neuronal sensitivity to ventral skin stimulation. The asymmetry between the sizes of ipsi and contralesional ventral RFs at 35 days was not observed for dorsal RFs. The ventral RF expansion was found as the animals displayed a predominant weight distribution on the ipsilesional hindlimb. The prominent RF enlargement led to a representational dedifferentiation of the cortical sectors of the map serving the ventral skin of the ipsilesional hindpaw. No such dedifferentiation was found for cortical areas representing dorsal skin territories. However, the total areal extent of the maps was not modified at this chronic stage of the lesion.

Immediate expansion of the cutaneous RFs of S1 neurons following UVN reveals modulatory effects of vestibular inputs on the somatosensory neuron responses.

Somatotopically organized responses to tactile stimulation are found in cells located throughout the ventral postero-medial (VPM, Diamond et al., 1992), ventral postero-lateral (VPL, Francis et al., 2008) nuclei and in S1, as has long been established. Interestingly, the vestibular nuclei complex also massively projects to the VPM and the VPL in rodents and humans (Nagata, 1986; Shiroyama et al., 1999; Lopez and Blanke, 2011 for review). Electrophysiological recordings have provided evidence that these thalamic nuclei respond not only to cutaneous or proprioceptive inputs, but also to vestibular stimulation (Deecke et al., 1977; Raymond et al., 1974; Sans et al., 1970; Wijesinghe et al., 2015). Furthermore, vestibular responses have also been recorded in the rodent somatosensory cortex (Leong et al., 2019; Rancz et al., 2015).

Given the above-mentioned anatomical and functional connectivity between the vestibular nuclei and the primary somatosensory cortex, the impact of the vestibular neurectomy on the S1 neuron activity was very likely to reveal crossmodal cortical interactions between somatosensory and vestibular inputs. Indeed, our electrophysiological mapping within the ipsi- and contralesional S1 cortex during the first hours after the UVN did show immediate cortical effects of the vestibular loss. The early expansion and shift in location of RFs reported herein are consistent with those found in previous studies of cortical reorganization after peripheral nerve injury (Navarro et al., 2007), amputation (Calford and Tweedale, 1988; Turnbull and Rasmusson, 1990), local anesthesia (Rossini et al., 1994), or epidural block (Metzler and Marks, 1979), which all demonstrate immediate shifting of cutaneous RFs for neurons located in the deafferented cortical zone. In the present study, the early postlesion RF enlargement was recorded in both hemispheres as early as the few hours after the lesion in the absence of behaviorally-induced changes, since the mapping procedure was initiated while the animal was still anesthetized. Interestingly, this alteration was mainly demonstrated for the ventral skin of the hindpaw, suggesting that the influence of vestibular inputs on S1 neurons is primarily on those representing the foot sole which is strongly involved in antigravity stance and postural control. Postlesion increase in ventral RF size led to a substantial remodeling of the hindpaw cutaneous maps. The vestibulo-thalamic projections observed in humans (Magnin and Kennedy, 1979; for review see Lopez and Blanke, 2011) and cats (Condé and Condé, 1978; Kotchabhakdi et al., 1980) have been described as bilateral with a contralateral predominance. As mentioned earlier, vestibular responses have also been recorded in the rodent somatosensory cortex (Leong et al., 2019; Rancz et al., 2015). However, these studies showed no quantitative difference in the amplitude of bilaterally recorded responses. Nonetheless, we found a greater expansion of ventral RFs on the contralesional hindpaw. This effect is in accordance with a study showing a dominance of the vestibular processing in the left hemisphere (Best et al., 2014) in which the contralesional hindpaw is represented in our study. Hence,

our findings, based on vestibular deafferentation, corroborate and extend this previous study, and suggest that vestibular signals that influence S1 neurons receiving cutaneous inputs contribute to perceptually guided posturo-locomotor adjustments.

Neuroplasticity mechanisms underlying immediate RFs enlargement following vestibular deafferentation

It is well documented that cortical maps are dynamically reshaped through ongoing adjustments in the balance of excitatory and inhibitory influences on their constituent neurons. Drastic and immediate deafferentation-induced disruption in this balance alters the RF properties of cortical neurons through weakening/strengthening of already existing thalamocortical and intracortical synapses, and thus rapidly remodels the functional circuitry of cortical networks (Harding-Forrester and Feldman, 2018; Xerri, 2012). As the vestibular deafferentation induces an electrophysiological imbalance between the vestibular nuclei characterized by increased excitability within the intact medial vestibular nuclei (Curthoys and Halmagyi, 1995; Smith and Curthoys, 1988), and given predominant contralateral vestibulo-thalamic projections, one could postulate that the excitatory vestibular inputs to the ipsilesional somatosensory cortex are potentiated. The resulting hyperexcitability of S1 neurons may thus lead to cutaneous RF enlargement predominantly on the contralesional hindpaw. Our findings corroborate this hypothesis, as contralesional hindpaw RFs were more enlarged after the UVN than were the ipsilesional. In addition, we found a higher neuronal sensitivity to cutaneous stimulation in the cortical area of the contralesional hindpaw.

Considering a non-exclusive alternative hypothesis, the postlesion RF enlargement might result from a rapid disinhibition process. Given the bilateral projections of vestibulo-thalamic inputs, the VN imbalance may be expected to result in decreased thalamo-cortical inputs on both S1 cortices, which would be consistent with the bilateral, however asymmetrical, effects of the UVN observed in our study. Therefore, we postulate that the immediate expansion of cutaneous RFs reveals a reduction of inhibition normally exerted by vestibular projections onto S1 layer IV neurons, possibly via thalamo-cortical inputs and/or cortico-cortical connections. Indeed, it has long been argued that intracortical inhibition plays a key role in controlling the spatial selectivity of cortical neurons through segregation of broad sets of converging thalamo-cortical synaptic inputs (see Calford, 2002; Jones, 1993; Xerri, 2012). Consistently, cutaneous RFs of somatosensory cortical neurons were enlarged when GABA-mediated local inhibition was antagonized by intracortical bicuculine injection (Alloway et al., 1989; Dykes et al., 1984; Tremere et al., 2001) whereas injection of baclofen, a

609 selective agonist for the $GABA_A$ receptors, induced a shrinkage of S1 neurons' cutaneous RFs
610 (Kyriazi et al., 1996). A release of afferent-driven intracortical tonic inhibition results in an enhanced
611 effectiveness of convergent cutaneous inputs. Therefore, this could be a most likely mechanism for
612 rapid unmasking of previously subthreshold afferent connections reflected by the rapid expansion of
613 cutaneous RFs of S1 neurons following the loss of tonic modulatory vestibular inputs.
614
615 To consider our data in the particular context of heteromodal sensory integration in primary
616 cortical areas, it is worth mentioning that auditory inputs to V1 were found to decrease visually
617 induced activity (Iurilli et al., 2012). Along the same lines, acute hearing loss was shown to release
618 the inhibitory effects of A1 neurons on visually elicited responses in V1 and lead to a concomitant
619 increase in V1 activation (Teichert and Bolz, 2017). However, the suppressive effect may be
620 functionally adapted, as additional data showed that auditory stimulation sharpens the orientation
621 selectivity of V1 neurons (Ibrahim et al., 2016). These data are in accordance with our findings on
622 the vestibular deafferentation acute effects on cutaneous RFs of S1 neurons. Collectively, the
623 available evidence supports the view that, in normal conditions, cross modal modulation may act to
624 improve the tuning of neuronal response properties in primary sensory cortices.
625
626 **The postural strategy leading to increased cutaneous feedback from the ipsilesional hindpaw**
627 **remodels S1 cutaneous neurons' responses**
628
629 One week after UVN, rats typically adopt a postural compensatory strategy to maintain their
630 posturo-locomotor stability, *i.e.* by shifting their body weight toward the ipsilesional paws. This
631 postural strategy has been reported in our previous studies (Marouane et al., 2020; Tighilet et al.,
632 2017) highlighting that weight distribution is a sensitive parameter for the assessment of the postural
633 syndrome in the UVN rodent model. The postural strategy which begins around day 7 and is
634 consistently maintained beyond the first month after the lesion may reflect the need for the rat to
635 better feel the ipsilesional limbs and increase tactilo-plantar feedback to achieve better antigravity
636 stance and postural control. Such a strategy is very likely to accentuate the tactilo-plantar flow from
637 the ipsilesional paws projecting to S1, and thus to create a functional asymmetry between the ipsi-
638 and contralesional hindlimb cortical areas during posturo-locomotor activities. In line with our
639 findings, stroke patients adopt a postural strategy by applying more weight on the non-impaired leg
640 to achieve better postural stability (Aruin et al., 2000; Mizrahi et al., 1989; Sackley, 1991). Thus, the
641 shift of body weight could represent a postural adaptive strategy following peripheral or central
642 damage.

Functional organization of somatotopic cortical areas is shaped by tactile experience (for reviews, Xerri 2008; Harding-Forrester and Feldman, 2018). Our data show a drastic remodeling of the ipsilesional hindpaw map due to a marked increase of the number of recording sites displaying enlarged ventral skin RFs (*mixed* areas) 35 days after UVN. This cortical remodeling disrupting the somatotopic arrangement of the cutaneous map led to a greater dedifferentiation of the hindlimb representation than that triggered in the few hours after the vestibular deafferentation. This finding is consistent with numerous studies showing a use-dependent recruitment of new cortical territories in S1, for more intensely or frequently stimulated skin surfaces, that is related to the translocation of the cutaneous RFs of constituent neurons over those skin territories. Furthermore, we reasoned that the asymmetrical tactilo-plantar stimulation of the hindpaws resulting from the shift in body weight would induce larger cutaneous surfaces temporally co-stimulated on the lesioned side. In line with this hypothesis, 35 days after the vestibular loss, we found a substantial expansion of cutaneous RFs covering the ventral skin surfaces of the ipsilesional hindpaw, whereas the RF size on the contralesional hindpaw were similar to those recorded prior to the lesion, thus leading to a strong interhemispheric asymmetry between ventral RFs. The neuronal sensitivity was also found to be asymmetric as the sensitivity in the ipsilesional hindpaw area tended to increase whereas that in the contralesional hindpaw area strongly decreased. These RF property changes are in accordance with the postural asymmetry.

One can assume that the reduced weight on the contralesional paws at rest and during locomotion was sufficient to maintain the organizational features of the cortical map. By contrast, the experience-driven expansion of cutaneous RFs over the ipsilesional hindpaw is likely to result from amalgamation of normally distinct thalamic RFs, as neurons displayed extracellular responses to new sets of inputs. Because of the simultaneous stimulation of larger cutaneous territories during posturo-locomotor activities after UVN, one can hypothesize that the over-reliance on the ipsilesional hindpaw was likely to generate cutaneous inputs spatially less restricted on a particular region of the paw. This postural modification led to temporally more coherent inputs because of the simultaneous stimulation of larger cutaneous territories during posturo-locomotor activities. This interpretation is supported by earlier studies showing the critical role of input timing in determining cortical map topologies and spatial resolution. These studies have revealed that locally synchronous cutaneous stimulation leads to an enlargement of S1 neurons' cutaneous RFs over co-stimulated digits in primate (Byl et al., 1996; Clark et al., 1988; Wang et al., 1995) and Human (Godde et al., 2003; Schwenkreis et al., 2001; Stavrinou et al., 2007), and for co-stimulated whiskers in the barrel cortex (Diamond et

al., 1993). An increase in RF size was also observed in adult rats exposed to hypergravity (2G) generated by a centrifuge during development, altering both proprioceptive and cutaneous inputs (Zennou-Azogui et al., 2016) as well as in rats housed in impoverished environment that reduced their exploratory behavior (Coq and Xerri, 1999; Godde et al., 2002). Furthermore, somatotopic maps can be remodeled after a few days of salient tactile experience modifying the spatio-temporal dynamics of input to S1, such as nursing (Rosselet et al., 2006; Xerri et al., 1994), forced use of the non-restricted forelimb in postural balance after unilateral forelimb immobilization (Coq and Xerri, 1999), or hypodynamia-hypokinesia (Canu et al., 2003; Dupont et al., 2003, 2001; Langlet et al., 1999).

At 35 days postlesion, we also noticed an enlargement of the ipsilesional dorsal RFs, as compared to intact rats. However, this alteration did not lead to asymmetrical RF sizes between ipsi- and contralesional hindpaws, contrary to the ventral RFs. Moreover, the increase in dorsal RFs was not accompanied by a dedifferentiation of the dorsal sectors of the cortical maps. The differential effect of the UVN on the ipsi- and contralesional RFs leading to a ventral skin RF expansion restricted to the ipsilesional hindpaw confirms the view of a postural effect on somatosensory cortical maps *i.e.*, an asymmetry between ventral RF sizes.

The ability to precisely localize tactile stimuli depends on the RF size of S1 neurons determining the grain of spatial representation and thus the representational differentiation of the body somatotopic maps. Accordingly, one can assume that the loss of vestibular inputs inducing an expansion and spatial shift of the cutaneous ventral RFs of S1 neurons has a strong impact on tactile discrimination abilities. In an attempt to reconcile our findings with those reported in the cited studies in healthy human participants, one can postulate that the loss of vestibular inputs strongly modulates the response characteristics of cortical somatosensory neurons, resulting in impaired spatial discrimination tactile abilities. Therefore, our findings indicate that crossmodal interplay between vestibular and cutaneous-plantar inputs within the primary somatosensory cortex contributes to modulate tactile discriminative abilities which may be crucial to optimally regulate posturo-locomotor activities. In line with this view, it has been shown that galvanic and caloric vestibular stimulation improves the ability to detect tactile stimuli applied on both hands of healthy participants (Ferrè et al., 2013, 2011a, 2011b).

Numerous studies support the crucial contribution of plantar cutaneous sensation and pressure feedback in the control of human stance and locomotion (Inglis et al., 2002; Kavounoudias et al.,

1998; Magnusson et al., 1990; Strzalkowski et al., 2018). For instance, plantar anesthesia increases instability during standing and walking (Fiolkowski et al., 2002).-We hypothesized that the behavioral strategy consisting in body weight shift to ipsilesional side is aimed at reinforcing somatosensory plantar feed-back to improve postural control, although RF size enlargement is detrimental to fine spatial tactile discrimination. In normal conditions, vestibular inputs may improve the tactile acuity on the plantar skin by refining the RF size of SI neurons, as indicated by the immediate RF enlargement induced by the UVN. Therefore, considering a potential clinical relevance of our findings, it is reasonable to assume that rehabilitative procedures (*e.g.* walking on a floor with different textures) aimed at enhancing spatial discrimination of plantar stimuli may improve posturo-locomotor adjustments in vestibulo-deficient patients.

Conclusion

The present study reveals for the first time that acute unilateral vestibular loss reshapes the cutaneous receptive fields of S1 neurons and, thereby, highlights the bilateral and asymmetrical modulatory influence of vestibular inputs on tactile processing related to posturo-locomotor balance control. The finding that the UVN induced an early expansion of the cortical cutaneous receptive fields reveals that vestibular influences contribute to maintaining a fine somatotopic organization of the foot sole cutaneous representation in S1. In addition, we suggest that the postural strategy consisting of a body shift to the lesioned side in order to improve posturo-locomotor balance in UVN rodents induces a use-dependent remodeling of the ipsilesional hindlimb cutaneous map at the chronic stage of the lesion (see **Figure 6** showing a schematic illustration of main effects of the UVN on S1 cortex). Further studies should evaluate the relative contribution of corticocortical and thalamocortical inputs to the modulatory influence of vestibular inputs on S1 neurons.

Declarations of interest

The authors declare no competing financial interests.

Funding

This research was supported by grants from the Ministère de l'Enseignement Supérieur et de la Recherche and CNRS (Aix-Marseille Université, UMR 7291). The Société Francophone Posture

Equilibre et Locomotion (SOFPEL) provided a travel grant (‘Bourse de voyage outre-atlantique de la Francophonie 2019’).

Acknowledgments

We thank Elodie Mansour and Jean Luc Fina for taking care of the animals, Nicolas Catz for designing the MAPCO software and Michael Paul for proofreading the English text.

Author Contributions

Supervision: C.X., B.T., Y.Z.A.; conceptualization and writing-original draft: G.R., J.F., C.X., B.T., Y.Z.A.; methodology and investigation: G.R., J.F., D.P., C.X., B.T., Y.Z.A.; statistical analysis: J.F., A.E.; writing – review & editing: G.R., J.F., C.X., B.T., Y.Z.A., A.E.

Bibliography

Alloway, K.D., Rosenthal, P., Burton, H., 1989. Quantitative measurements of receptive field changes during antagonism of GABAergic transmission in primary somatosensory cortex of cats. Exp Brain Res 78, 514–532. https://doi.org/10.1007/BF00230239

Aruin, A.S., Hanke, T., Chaudhuri, G., Harvey, R., Rao, N., 2000. Compelled weightbearing in persons with hemiparesis following stroke: the effect of a lift insert and goal-directed balance exercise. J Rehabil Res Dev 37, 65–72

Bense, S., Bartenstein, P., Lochmann, M., Schlindwein, P., Brandt, T., Dieterich, M., 2004. Metabolic changes in vestibular and visual cortices in acute vestibular neuritis. Ann. Neurol. 56, 624–630. https://doi.org/10.1002/ana.20244

Best, C., Lange, E., Buchholz, H.G. Schreckenberger, M., Reuss, S., Dieterich, M., 2014. Left hemispheric dominance of vestibular processing indicates lateralization of cortical functions in rats. Brain Struct Funct. 219(6):2141-58. doi: 10.1007/s00429-013-0628-1

Borel, L., Lacour, M., 1992. Functional coupling of the stabilizing eye and head reflexes during horizontal and vertical linear motion in the cat. Exp Brain Res 91, 191–206. https://doi.org/10.1007/BF00231654

Brandt, T., Dieterich, M., 2019. Thalamocortical network: a core structure for integrative multimodal vestibular functions. Current Opinion in Neurology 32, 154–164. https://doi.org/10.1097/WCO.0000000000000638

Byl, N.N., Merzenich, M.M., Jenkins, W.M., 1996. A primate genesis model of focal dystonia and repetitive strain injury: I. Learning-induced dedifferentiation of the representation of the hand in the primary somatosensory cortex in adult monkeys. Neurology 47, 508–520. https://doi.org/10.1212/wnl.47.2.508

Calford, M.B., 2002. Dynamic representational plasticity in sensory cortex. Neuroscience 111, 709–738. https://doi.org/10.1016/s0306-4522(02)00022-2

784 Calford, M.B., Tweedale, R., 1988. Immediate and chronic changes in responses of somatosensory
785 cortex in adult flying-fox after digit amputation. Nature 332, 446–448.
786 https://doi.org/10.1038/332446a0
787 Canu, M.H., Langlet, C., Dupont, E., Falempin, M., 2003. Effects of hypodynamia-hypokinesia on
788 somatosensory evoked potentials in the rat. Brain Res. 978, 162–168.
789 https://doi.org/10.1016/s0006-8993(03)02804-x
790 Canu, M.-H., Stevens, L., Falempin, M., 2007. Effect of hindlimb suspension on activation and MHC
791 content of triceps brachii and on the representation of forepaw on the sensorimotor cortex.
792 Exp. Neurol. 203, 521–530. https://doi.org/10.1016/j.expneurol.2006.09.005
793 Carriot, J., Jamali, M., Cullen, K.E., 2015. Rapid adaptation of multisensory integration in vestibular
794 pathways. Front Syst Neurosci 9, 59. https://doi.org/10.3389/fnsys.2015.00059
795 Charbonneau, V., Laramée, M.-E., Boucher, V., Bronchti, G., Boire, D., 2012. Cortical and
796 subcortical projections to primary visual cortex in anophthalmic, enucleated and sighted mice.
797 Eur. J. Neurosci. 36, 2949–2963. https://doi.org/10.1111/j.1460-9568.2012.08215.x
798 Clark, S.A., Allard, T., Jenkins, W.M., Merzenich, M.M., 1988. Receptive fields in the body-surface
799 map in adult cortex defined by temporally correlated inputs. Nature 332, 444–445.
800 https://doi.org/10.1038/332444a0
801 Condé, F., Condé, H., 1978. Thalamic projections of the vestibular nuclei in the cat as revealed by
802 retrograde transport of horseradish peroxidase. Neurosci. Lett. 9, 141–146.
803 https://doi.org/10.1016/0304-3940(78)90062-9
804 Coq, J.O., Xerri, C., 1999. Acute reorganization of the forepaw representation in the rat SI cortex
805 after focal cortical injury: neuroprotective effects of piracetam treatment. Eur. J. Neurosci. 11,
806 2597–2608. https://doi.org/10.1046/j.1460-9568.1999.00673.x
807 Coq, J.O., Xerri, C., 1998. Environmental enrichment alters organizational features of the forepaw
808 representation in the primary somatosensory cortex of adult rats. Exp Brain Res 121, 191–
809 204. https://doi.org/10.1007/s002210050452
810 Curthoys, I.S., Halmagyi, G.M., 1995. Vestibular compensation: a review of the oculomotor, neural,
811 and clinical consequences of unilateral vestibular loss. Journal of vestibular research :
812 equilibrium & orientation 5, 67–107.
813 Darlington, C.L., Smith, P.F., 2000. Molecular mechanisms of recovery from vestibular damage in
814 mammals: recent advances. Progress in Neurobiology 62, 313–325.
815 https://doi.org/10.1016/S0301-0082(00)00002-2
816 Deecke, L., Schwarz, D.W.F., Fredrickson, J.M., 1977. Vestibular responses in the Rhesus monkey
817 ventroposterior thalamus. II. Vestibulo-proprioceptive convergence at thalamic neurons.
818 Experimental Brain Research 30–30. https://doi.org/10.1007/BF00237252.
819 Diamond, M.E., Armstrong-James, M., Ebner, F.F. 1992. Somatic sensory responses in the rostral
820 sector of the posterior group (POm) and in the ventral posterior medial nucleus (VPM) of the
821 rat thalamus. J Comp Neurol. 1992 Apr 22;318(4):462-76. doi: 10.1002/cne.903180410
822 Diamond, M.E., Armstrong-James, M., Ebner, F.F., 1993. Experience-dependent plasticity in adult
823 rat barrel cortex. Proc. Natl. Acad. Sci. U.S.A. 90, 2082–2086.
824 https://doi.org/10.1073/pnas.90.5.2082
825 Dupont, E., Canu, M.-H., Falempin, M., 2003. A 14-day period of hindpaw sensory deprivation
826 enhances the responsiveness of rat cortical neurons. Neuroscience 121, 433–439.
827 https://doi.org/10.1016/s0306-4522(03)00494-9
828 Dupont, E., Canu, M.H., Langlet, C., Falempin, M., 2001. Time course of recovery of the
829 somatosensory map following hindpaw sensory deprivation in the rat. Neurosci. Lett. 309,
830 121–124. https://doi.org/10.1016/s0304-3940(01)02050-x
831 Dutheil, S., Watabe, I., Sadlaoud, K., Tonetto, A., Tighilet, B., 2016. BDNF signaling promotes
832 vestibular compensation by increasing neurogenesis and remodeling the expression of

potassium-chloride cotransporter KCC2 and GABAA receptor in the vestibular nuclei. Journal of Neuroscience 36, 6199–6212.
Dykes, R.W., Landry, P., Metherate, R., Hicks, T.P., 1984. Functional role of GABA in cat primary somatosensory cortex: shaping receptive fields of cortical neurons. J. Neurophysiol. 52, 1066–1093. https://doi.org/10.1152/jn.1984.52.6.1066
Ferrè, E.R., Bottini, G., Haggard, P., 2011a. Vestibular modulation of somatosensory perception: Vestibular modulation of somatosensory perception. European Journal of Neuroscience 34, 1337–1344. https://doi.org/10.1111/j.1460-9568.2011.07859.x
Ferrè, E.R., Day, B.L., Bottini, G., Haggard, P., 2013. How the vestibular system interacts with somatosensory perception: A sham-controlled study with galvanic vestibular stimulation. Neurosci Lett 550, 35–40. https://doi.org/10.1016/j.neulet.2013.06.046
Ferrè, E.R., Sedda, A., Gandola, M., Bottini, G., 2011b. How the vestibular system modulates tactile perception in normal subjects: a behavioural and physiological study. Exp Brain Res 208, 29–38. https://doi.org/10.1007/s00221-010-2450-9
Festing, M.F., 2006 .Design and statistical methods in studies using animal models of development. ILAR J 47(1): 5-14.
Festing, M.F., Altman, D.G., 2002. Guidelines for the design and statistical analysis of experiments using laboratory animals. ILAR Journal 43(4): 244-258
Fiolkowski, P., Brunt, D., Bishop, M., Woo, R., 2002. Does postural instability affect the initiation of human gait? Neurosci. Lett. 323, 167–170. https://doi.org/10.1016/s0304-3940(02)00158-1
Francis, J.T., Xu, S., Chapin, J.K., 2008 Proprioceptive and cutaneous representations in the rat ventral posterolateral thalamus. J Neurophysiol. 99(5):2291-304. https://doi.org/10.1152/jn.01206.2007
Godde, B., Berkefeld, T., David-Jürgens, M., Dinse, H.R., 2002. Age-related changes in primary somatosensory cortex of rats: evidence for parallel degenerative and plastic-adaptive processes. Neurosci Biobehav Rev 26, 743–752. https://doi.org/10.1016/s0149-7634(02)00061-1
Godde, B., Ehrhardt, J., Braun, C., 2003. Behavioral significance of input-dependent plasticity of human somatosensory cortex. Neuroreport 14, 543–546. https://doi.org/10.1097/00001756-200303240-00002
Greer, T., Dunlap, W.P. 1997. Analysis of variance with ipsative measures. Psychol Methods 2: 200
Harding-Forrester, S., Feldman, D.E., 2018. Somatosensory maps. Handb Clin Neurol 151, 73–102. https://doi.org/10.1016/B978-0-444-63622-5.00004-8
Helmchen, C., Klinkenstein, J., Machner, B., Rambold, H., Mohr, C., Sander, T., 2009. Structural changes in the human brain following vestibular neuritis indicate central vestibular compensation. Ann. N. Y. Acad. Sci. 1164, 104–115. https://doi.org/10.1111/j.1749-6632.2008.03745.x
Henschke, J.U., Noesselt, T., Scheich, H., Budinger, E., 2015. Possible anatomical pathways for short-latency multisensory integration processes in primary sensory cortices. Brain Struct Funct 220, 955–977. https://doi.org/10.1007/s00429-013-0694-4
Horak, F.B., 2009. Postural Compensation for Vestibular Loss. Annals of the New York Academy of Sciences 1164, 76–81. https://doi.org/10.1111/j.1749-6632.2008.03708.x
Horak, F.B., Nashner, L.M., Diener, H.C., 1990. Postural strategies associated with somatosensory and vestibular loss. Exp Brain Res 82, 167–177. https://doi.org/10.1007/BF00230848
Hubel, D.H., Wiesel, T.N., 1964. Effects of monocular deprivation in kittens. Naunyn-Schmiedebergs Arch. exp. Path. u. Pharmak. 248, 492–497. https://doi.org/10.1007/BF00348878
Ibrahim, L.A., Mesik, L., Ji, X., Fang, Q., Li, H., Li, Y., Zingg, B., Zhang, L.I., Tao, H.W., 2016. Cross-modality Sharpening of Visual Cortical Processing through Layer 1-Mediated

Inhibition and Disinhibition. Neuron 89, 1031–1045. https://doi.org/10.1016/j.neuron.2016.01.027
Inglis, J.T., Kennedy, P.M., Wells, C., Chua, R., 2002. The Role of Cutaneous Receptors in the Foot, in: Gandevia, S.C., Proske, U., Stuart, D.G. (Eds.), Sensorimotor Control of Movement and Posture, Advances in Experimental Medicine and Biology. Springer US, Boston, MA, pp. 111–117. https://doi.org/10.1007/978-1-4615-0713-0_14
Iurilli, G., Ghezzi, D., Olcese, U., Lassi, G., Nazzaro, C., Tonini, R., Tucci, V., Benfenati, F., Medini, P., 2012. Sound-driven synaptic inhibition in primary visual cortex. Neuron 73, 814–828. https://doi.org/10.1016/j.neuron.2011.12.026
Jamali, M., Mitchell, D.E., Dale, A., Carriot, J., Sadeghi, S.G., Cullen, K.E., 2014. Neuronal detection thresholds during vestibular compensation: contributions of response variability and sensory substitution: Neuronal detection thresholds during vestibular compensation. The Journal of Physiology 592, 1565–1580. https://doi.org/10.1113/jphysiol.2013.267534
Jenkins, W.M., Merzenich, M.M., Ochs, M.T., Allard, T., Guíc-Robles, E., 1990. Functional reorganization of primary somatosensory cortex in adult owl monkeys after behaviorally controlled tactile stimulation. J. Neurophysiol. 63, 82–104. https://doi.org/10.1152/jn.1990.63.1.82
Jones, E.G., 1993. GABAergic neurons and their role in cortical plasticity in primates. Cereb Cortex 3, 361–372. https://doi.org/10.1093/cercor/3.5.361-a
Kavounoudias, A., Roll, R., Roll, J.P., 1998. The plantar sole is a “dynamometric map” for human balance control. Neuroreport 9, 3247–3252. https://doi.org/10.1097/00001756-199810050-00021
Kotchabhakdi, N., Rinvik, E., Walberg, F., Yingchareon, K., 1980. The vestibulothalamic projections in the cat studied by retrograde axonal transport of horseradish peroxidase. Exp Brain Res 40, 405–418. https://doi.org/10.1007/BF00236149
Kyriazi, H.T., Carvell, G.E., Brumberg, J.C., Simons, D.J., 1996. Effects of baclofen and phaclofen on receptive field properties of rat whisker barrel neurons. Brain Res. 712, 325–328. https://doi.org/10.1016/0006-8993(95)01562-0
Lacour, M., Borel, L., 1993. Vestibular control of posture and gait. Arch Ital Biol 131, 81–104.
Lacour, M., Tighilet, B., 2010. Plastic events in the vestibular nuclei during vestibular compensation: The brain orchestration of a “deafferentation” code. Restorative Neurology and Neuroscience 28, 19–35. https://doi.org/10.3233/RNN-2010-0509
Langlet, C., Canu, M.H., Falempin, M., 1999. Short-term reorganization of the rat somatosensory cortex following hypodynamia-hypokinesia. Neurosci. Lett. 266, 145–148. https://doi.org/10.1016/s0304-3940(99)00296-7
Leong, A.T.L., Gu, Y., Chan, Y.-S., Zheng, H., Dong, C.M., Chan, R.W., Wang, X., Liu, Y., Tan, L.H., Wu, E.X., 2019. Optogenetic fMRI interrogation of brain-wide central vestibular pathways. Proc Natl Acad Sci USA 116, 10122–10129. https://doi.org/10.1073/pnas.1812453116
Liberge, M., Manrique, C., Bernard-Demanze, L., Lacour, M., 2010. Changes in TNFα, NFκB and MnSOD protein in the vestibular nuclei after unilateral vestibular deafferentation. Journal of Neuroinflammation 7, 91. https://doi.org/10.1186/1742-2094-7-91
Lopez, C., 2016. The vestibular system: balancing more than just the body. Current Opinion in Neurology 29, 74–83. https://doi.org/10.1097/WCO.0000000000000286
Lopez, C., Blanke, O., 2011. The thalamocortical vestibular system in animals and humans. Brain Research Reviews 67, 119–146. https://doi.org/10.1016/j.brainresrev.2010.12.002
Luccarini, P., Gahery, Y., Blanchet, G., Pompeiano, O., 1992. GABA receptors in Deiters nucleus modulate posturokinetic responses to cortical stimulation in the cat. Arch Ital Biol 130, 127–154.

Magnin, M., Kennedy, H., 1979. Anatomical evidence of a third ascending vestibular pathway involving the ventral lateral geniculate nucleus and the intralaminar nuclei of the cat. Brain Res. 171, 523–529. https://doi.org/10.1016/0006-8993(79)91056-4

Magnusson, M., Enbom, H., Johansson, R., Pyykkö, I., 1990. The Importance of Somatosensory Information from Feet in Postural Control in Man. Disorder of Posture and Gait 1990.

Marouane, E., Rastoldo, G., El Mahmoudi, N., Péricat, D., Chabbert, C., Artzner, V., Tighilet, B., 2020. Identification of New Biomarkers of Posturo-Locomotor Instability in a Rodent Model of Vestibular Pathology. Front. Neurol. 11. https://doi.org/10.3389/fneur.2020.00470

Massé, I.O., Ross, S., Bronchti, G., Boire, D., 2017. Asymmetric Direct Reciprocal Connections Between Primary Visual and Somatosensory Cortices of the Mouse. Cereb. Cortex 27, 4361–4378. https://doi.org/10.1093/cercor/bhw239

Mead, R. 1988. The design of experiments. Cambridge, New York: Cambridge University Press. 620 p

Merzenich, M.M., Kaas, J.H., Wall, J., Nelson, R.J., Sur, M., Felleman, D., 1983. Topographic reorganization of somatosensory cortical areas 3b and 1 in adult monkeys following restricted deafferentation. Neuroscience 8, 33–55. https://doi.org/10.1016/0306-4522(83)90024-6

Metzler, J., Marks, P.S., 1979. Functional changes in cat somatic sensory-motor cortex during short-term reversible epidural blocks. Brain Res. 177, 379–383. https://doi.org/10.1016/0006-8993(79)90790-x

Mizrahi, J., Solzi, P., Ring, H., Nisell, R., 1989. Postural stability in stroke patients: vectorial expression of asymmetry, sway activity and relative sequence of reactive forces. Med Biol Eng Comput 27, 181–190. https://doi.org/10.1007/BF02446228

Nagata, S., 1986. The vestibulothalamic connections in the rat: a morphological analysis using wheat germ agglutinin-horseradish peroxidase. Brain Res. 376, 57–70. https://doi.org/10.1016/0006-8993(86)90899-1

Navarro, X., Vivó, M., Valero-Cabré, A., 2007. Neural plasticity after peripheral nerve injury and regeneration. Prog. Neurobiol. 82, 163–201. https://doi.org/10.1016/j.pneurobio.2007.06.005

Péricat, D., Farina, A., Agavnian-Couquiaud, E., Chabbert, C., Tighilet, B., 2017. Complete and irreversible unilateral vestibular loss: A novel rat model of vestibular pathology. Journal of Neuroscience Methods 283, 83–91. https://doi.org/10.1016/j.jneumeth.2017.04.001

Polley, D.B., Kvasnák, E., Frostig, R.D., 2004. Naturalistic experience transforms sensory maps in the adult cortex of caged animals. Nature 429, 67–71. https://doi.org/10.1038/nature02469

Rancz, E.A., Moya, J., Drawitsch, F., Brichta, A.M., Canals, S., Margrie, T.W., 2015. Widespread Vestibular Activation of the Rodent Cortex. J. Neurosci. 35, 5926–5934. https://doi.org/10.1523/JNEUROSCI.1869-14.2015

Rastoldo, G., El Mahmoudi, N., Marouane, E., Pericat, D., Watabe, I., Toneto, A., López-Juárez, A., Chabbert, C., Tighilet, B., 2021. Adult and endemic neurogenesis in the vestibular nuclei after unilateral vestibular neurectomy. Prog Neurobiol 196, 101899. https://doi.org/10.1016/j.pneurobio.2020.101899

Raymond, J., Sans, A., Marty, R., 1974. [Thalamic projections of the vestibular nuclei: a histological study in the cat (author's transl)]. Exp Brain Res 20, 273–283. https://doi.org/10.1007/BF00238317

Robertson, D., Irvine, D.R., 1989. Plasticity of frequency organization in auditory cortex of guinea pigs with partial unilateral deafness. J. Comp. Neurol. 282, 456–471. https://doi.org/10.1002/cne.902820311

Rosselet, C., Zennou-Azogui, Y., Xerri, C., 2006. Nursing-induced somatosensory cortex plasticity: temporally decoupled changes in neuronal receptive field properties are accompanied by modifications in activity-dependent protein expression. J. Neurosci. 26, 10667–10676. https://doi.org/10.1523/JNEUROSCI.3253-06.2006

Rossini, P.M., Martino, G., Narici, L., Pasquarelli, A., Peresson, M., Pizzella, V., Tecchio, F., Torrioli, G., Romani, G.L., 1994. Short-term brain "plasticity" in humans: transient finger representation changes in sensory cortex somatotopy following ischemic anesthesia. Brain Res. 642, 169–177. https://doi.org/10.1016/0006-8993(94)90919-9

Sackley, C.M., 1991. Falls, sway, and symmetry of weight-bearing after stroke. Int Disabil Stud 13, 1–4. https://doi.org/10.3109/03790799109166267

Sadeghi, S.G., Minor, L.B., Cullen, K.E., 2012. Neural correlates of sensory substitution in vestibular pathways following complete vestibular loss. J. Neurosci. 32, 14685–14695. https://doi.org/10.1523/JNEUROSCI.2493-12.2012

Sadeghi, S.G., Minor, L.B., Cullen, K.E., 2011. Multimodal integration after unilateral labyrinthine lesion: single vestibular nuclei neuron responses and implications for postural compensation. J. Neurophysiol. 105, 661–673. https://doi.org/10.1152/jn.00788.2010

Sadeghi, S.G., Minor, L.B., Cullen, K.E., 2010. Neural correlates of motor learning in the vestibulo-ocular reflex: dynamic regulation of multimodal integration in the macaque vestibular system. J. Neurosci. 30, 10158–10168. https://doi.org/10.1523/JNEUROSCI.1368-10.2010

Sanes, J.N., Suner, S., Donoghue, J.P., 1990. Dynamic organization of primary motor cortex output to target muscles in adult rats. I. Long-term patterns of reorganization following motor or mixed peripheral nerve lesions. Exp Brain Res 79, 479–491. https://doi.org/10.1007/BF00229318

Sans, A., Raymond, J., Marty, R., 1970. Réponses thalamiques et corticales à la stimulation électrique du nerf vestibulaire chez le Chat. Exp Brain Res 10, 265–275. https://doi.org/10.1007/BF00235050

Scheirer, J., Ray, W.S., Hare, N. 1976. The analysis of ranked data derived from completely randomized factorial designs. Biometrics. 32 (2), 429-434.

Schwenkreis, P., Pleger, B., Höffken, O., Malin, J.P., Tegenthoff, M., 2001. Repetitive training of a synchronised movement induces short-term plastic changes in the human primary somatosensory cortex. Neurosci. Lett. 312, 99–102. https://doi.org/10.1016/s0304-3940(01)02196-6

Shiroyama, T., Kayahara, T., Yasui, Y., Nomura, J., Nakano, K., 1999. Projections of the vestibular nuclei to the thalamus in the rat: a Phaseolus vulgaris leucoagglutinin study. J Comp Neurol 407, 318–332.

Shupert, C.L., Horak, F.B., Black, F.O., 1994. Hip sway associated with vestibulopathy. J Vestib Res 4, 231–244.

Smith, P.F., Curthoys, I.S., 1989. Mechanisms of recovery following unilateral labyrinthectomy: a review. Brain Research Reviews 14, 155–180. https://doi.org/10.1016/0165-0173(89)90013-1

Stavrinou, M.L., Della Penna, S., Pizzella, V., Torquati, K., Cianflone, F., Franciotti, R., Bezerianos, A., Romani, G.L., Rossini, P.M., 2007. Temporal dynamics of plastic changes in human primary somatosensory cortex after finger webbing. Cereb. Cortex 17, 2134–2142. https://doi.org/10.1093/cercor/bhl120

Stiles, L., Smith, P.F., 2015. The vestibular-basal ganglia connection: balancing motor control. Brain Res. 1597, 180–188. https://doi.org/10.1016/j.brainres.2014.11.063

Strzalkowski, N.D.J., Peters, R.M., Inglis, J.T., Bent, L.R., 2018. Cutaneous afferent innervation of the human foot sole: what can we learn from single-unit recordings? Journal of Neurophysiology 120, 1233–1246. https://doi.org/10.1152/jn.00848.2017

Teichert, M., Bolz, J., 2018. How Senses Work Together: Cross-Modal Interactions between Primary Sensory Cortices. Neural Plast. 2018, 5380921. https://doi.org/10.1155/2018/5380921

Teichert, M., Bolz, J., 2017. Simultaneous intrinsic signal imaging of auditory and visual cortex reveals profound effects of acute hearing loss on visual processing. Neuroimage 159, 459–472. https://doi.org/10.1016/j.neuroimage.2017.07.037

Tighilet, B., Leonard, J., Mourre, C., Chabbert, C., 2019. Apamin treatment accelerates equilibrium recovery and gaze stabilization in unilateral vestibular neurectomized cats: Cellular and behavioral aspects. Neuropharmacology 144, 133–142. https://doi.org/10.1016/j.neuropharm.2018.10.029

Tighilet, B., Léonard, J., Watabe, I., Bernard-Demanze, L., Lacour, M., 2018. Betahistine Treatment in a Cat Model of Vestibular Pathology: Pharmacokinetic and Pharmacodynamic Approaches. Frontiers in Neurology 9. https://doi.org/10.3389/fneur.2018.00431

Tighilet, B., Péricat, D., Frelat, A., Cazals, Y., Rastoldo, G., Boyer, F., Dumas, O., Chabbert, C., 2017. Adjustment of the dynamic weight distribution as a sensitive parameter for diagnosis of postural alteration in a rodent model of vestibular deficit. PloS one 12, e0187472.

Tjernström, F., Zur, O., Jahn, K., 2016. Current concepts and future approaches to vestibular rehabilitation. J Neurol 263, 65–70. https://doi.org/10.1007/s00415-015-7914-1

Tremere, L., Hicks, T.P., Rasmusson, D.D., 2001. Expansion of receptive fields in raccoon somatosensory cortex in vivo by GABA(A) receptor antagonism: implications for cortical reorganization. Exp Brain Res 136, 447–455. https://doi.org/10.1007/s002210000612

Turnbull, B.G., Rasmusson, D.D., 1990. Acute effects of total or partial digit denervation on raccoon somatosensory cortex. Somatosens Mot Res 7, 365–389. https://doi.org/10.3109/08990229009144714

Wang, X., Merzenich, M.M., Sameshima, K., Jenkins, W.M., 1995. Remodelling of hand representation in adult cortex determined by timing of tactile stimulation. Nature 378, 71–75. https://doi.org/10.1038/378071a0

Waters, R.S., Li, C.X., McCandlish, C.A., 1995. Relationship between the organization of the forepaw barrel subfield and the representation of the forepaw in layer IV of rat somatosensory cortex. Exp Brain Res 103, 183–197. https://doi.org/10.1007/BF00231705

Welker, W., Sanderson, K.J., Shambes, G.M., 1984. Patterns of afferent projections to transitional zones in the somatic sensorimotor cerebral cortex of albino rats. Brain Res. 292, 261–267. https://doi.org/10.1016/0006-8993(84)90762-5

Wijesinghe, R., Protti, D.A., Camp, A.J., 2015. Vestibular Interactions in the Thalamus. Front Neural Circuits 9, 79. https://doi.org/10.3389/fncir.2015.00079

Xerri, C., 2012. Plasticity of cortical maps: multiple triggers for adaptive reorganization following brain damage and spinal cord injury. Neuroscientist 18, 133–148. https://doi.org/10.1177/1073858410397894

Xerri, C., 2008. Imprinting of idyosyncratic experience in cortical sensory maps: Neural substrates of representational remodeling and correlative perceptual changes. Behavioural Brain Research 192, 26–41. https://doi.org/10.1016/j.bbr.2008.02.038

Xerri, C., Zennou-Azogui, Y. 2021. Interplay between primary cortical areas and crossmodal plasticity, in Neural Connectivity. Heinbockel T (ed). IntechOpen. http://dx.doi.org/10.5772/intechopen.95450

Xerri, C., Bourgeon, S., Coq, J.-O., 2005. Perceptual context-dependent remodeling of the forepaw map in the SI cortex of rats trained on tactile discrimination. Behav. Brain Res. 162, 207–221. https://doi.org/10.1016/j.bbr.2005.03.003

Xerri, C., Coq, J.O., Merzenich, M.M., Jenkins, W.M., 1996. Experience-induced plasticity of cutaneous maps in the primary somatosensory cortex of adult monkeys and rats. J. Physiol. Paris 90, 277–287. https://doi.org/10.1016/s0928-4257(97)81438-6

Xerri, C., Gianni, S., Manzoni, D., Pompeiano, O., 1983. Central compensation of vestibular deficits. I. Response characteristics of lateral vestibular neurons to roll tilt after ipsilateral labyrinth deafferentation. Journal of Neurophysiology 50, 428–448. https://doi.org/10.1152/jn.1983.50.2.428

Xerri, C., Merzenich, M.M., Jenkins, W., Santucci, S., 1999. Representational plasticity in cortical area 3b paralleling tactual-motor skill acquisition in adult monkeys. Cereb. Cortex 9, 264–276. https://doi.org/10.1093/cercor/9.3.264

Xerri, C., Stern, J., Merzenich, M., 1994. Alterations of the cortical representation of the rat ventrum induced by nursing behavior. J Neurosci 14, 1710–1721. https://doi.org/10.1523/JNEUROSCI.14-03-01710.1994

Zennou-Azogui, Y., Borel, L., Lacour, M., Ez-Zaher, L., Ouaknine, M., 1993. Recovery of Head Postural Control Following Unilateral Vestibular Neurectomy in the Cat: Neck Muscle Activity and Neuronal Correlates in Deiters' Nuclei. Acta Oto-Laryngologica 113, 5–19. https://doi.org/10.3109/00016489309130556

Zennou-Azogui, Y., Catz, N., Xerri, C., 2016. Hypergravity within a critical period impacts on the maturation of somatosensory cortical maps and their potential for use-dependent plasticity in the adult. J. Neurophysiol. 115, 2740–2760. https://doi.org/10.1152/jn.00900.2015

Zwergal, A., Schlichtiger, J., Xiong, G., Beck, R., Günther, L., Schniepp, R., Schöberl, F., Jahn, K., Brandt, T., Strupp, M., Bartenstein, P., Dieterich, M., Dutia, M.B., la Fougère, C., 2016. Sequential [(18)F]FDG μPET whole-brain imaging of central vestibular compensation: a model of deafferentation-induced brain plasticity. Brain Struct Funct 221, 159–170. https://doi.org/10.1007/s00429-014-0899-1

Figure 1

Experimental protocol for evaluating postural deficits and remodeling of hindpaw cutaneous cortical maps after unilateral vestibular neurectomy (UVN).

A: Vestibular score and support surface assessment were performed one day before unilateral vestibular neurectomy (UVN) in the 1H and D35 groups and 1, 2, 3, 7, 10, 14, 21, 30 days after UVN in the latter group. Body weight distribution was also assessed prior to UVN, and before cortical mapping in all groups, including the controls (CTRL). Cortical mapping was initiated over the first hours following the lesion in the 1H group, and 35 days later in the D35 group. **B-C:** Schematic cortical mapping procedure. In each group, cortical recordings (about 60 sites per map; C1) were performed in layer IV either in the ipsilesional ($1H_{ipsi}$; $D35_{ipsi}$) or contralesional ($1H_{cont}$; $D35_{cont}$) hindpaw representational zone of S1 to determine the location and size of the neurons' cutaneous receptive fields (RFs). The RF nomenclature indicate their location on the hindpaw skin surface (C2). An example of a RF recorded in the *mixed* cortical area is represented by an orange circle including digits 3 and 4 and part of the plantar skin. Collection of all RFs recorded in a mapping session (C3) in order to generate a somatotopic cortical map (C4). **D:** Illustration of the device (DWB1®, Bioseb, France) used for dynamic weight-bearing assessment. The animal was placed in a plexiglass chamber (25 x 25 cm) and moved freely on a floor covered by a plate equipped with 2 000 force sensors. The animal behavior was videotaped and the distribution of its body weight on each of the four limbs was calculated offline (Marouane et al., 2020; Tighilet et al., 2017). **E:** The polygon in blue illustrates the body support surface measured during static state.

Figure 2

Effect of the UVN on the body weight distribution on the hindpaws.

A: Vestibular score profile illustrating the time course of behavioral syndrome over postlesion days (D). **B:** Time course of body support surface. **C:** Histograms illustrating the percentage of body mass applied on the hindpaws (in red, ipsilesional *left hindpaw*; in green, contralesional *right hindpaw*) before (Pre-op) and 35 days after UVN (D35). **D:** Histograms illustrating the percentage of body mass applied on the ipsilesional hindpaw in bipedal (yellow) or quadrupedal (blue) stance before and 35 days after the lesion. **: $P < 0.01$; ***: $P < 0.001$; ****: $P < 0.0001$, for comparisons with control values. All data are expressed as means ± SEM.

Figure 3

Impact of the UVN on the size of hindpaw cutaneous receptive fields (RFs) of S1 neurons.

A: Typical RFs located on the hindpaw glabrous (top) and hairy (bottom) skin surfaces of an intact rat (CTRL, left panel), and on the ipsilesional (Ipsi) and contralesional (Cont) hindpaws, recorded one hour (1H, middle panel), and 35 days (D35, right panel) after the lesion, in two rats. **B:** Mean relative size of all RFs (ventral, dorsal and ventral & dorsal) obtained in CTRL and UVN rats. Boxplots represent the first and the third quartiles and medians, while black dots individual outlier values. Red triangles show mean RF size. **C-D:** Relative size of ventral and dorsal skin RFs taken from the data shown in B. Horizontally aligned * and bars show statistical differences between the experimental groups. Statistical analyses were performed using Kruskal Wallis and Scheirer-Ray-Hare tests followed by Dunn *post-hoc* tests. *: $P < 0.05$; **: $P < 0.01$; ***: $P < 0.001$; ****: $P < 0.0001$.

Figure 4

Neuronal responsiveness to stimulation of the hindpaw ventral skin surfaces.

A: Mechanical thresholds of neuronal responses to stimulation of hindpaw ventral skin (*i.e.*, of ventral and ventral &dorsal RFs) obtained using von Frey monofilaments (bending pressures, g/mm^2), taken as measures of neuronal response sensitivity. Red triangles represent the average threshold for each experimental group, boxplots represent first and third quartiles and medians, while black dots show

individual threshold outlier values. Horizontally aligned * and bars show statistical differences between the experimental groups. Statistical analyses were performed using Kruskal Wallis and Scheirer-Ray-Hare tests followed by Dunn *post-hoc* tests. *: $P < 0.05$; **: $P < 0.01$; ***: $P < 0.001$; ****: $P < 0.0001$. **B:** Correlation between RF size and neuronal sensitivity plotted with a log-log scale (ANCOVA analysis, see Methods).

Figure 5

Remodeling of hindpaw cutaneous representational maps after UVN.

A: Representative electrophysiological cortical maps recorded from an intact rat (CTRL: left panel) and lesioned rats in which ipsilesional or contralesional hindpaw maps were obtained 1 hour (1H: middle panels) and 35 days (D35: right panels) after UVN. Note the postlesion striking changes in the proportion and topographic order of each representational zone, leading to a substantial dedifferentiation of the somatotopic maps. This effect was found in both ipsi- and contralesional hindpaw representations one hour after UVN, but only in ipsilesional hindpaw maps 35 days later. **B:** Boxplot showing the mean total map size in each group (mm^2). Boxplots illustrate the first and third quartiles and the median values, while black dots individual map size outlier values. **C:** Stacked histograms illustrating the relative mean areas of the different map regions, normalized with respect to the total hindlimb cortical area. These relative areas are color-coded (green: *simple* area in which cutaneous RFs were confined on individual digits and plantar pads; purple: *mixed* area corresponding to neurons with RFs localized on two or more hindpaw skin subdivisions; yellow: ventral *paw* area in which RFs included the whole ventral or dorsal paw surface). **D-E:** Separate distributions of ventral and dorsal skin RFs in each size category. Mean values of normalized map sectors are illustrated separately for ventral (D) and dorsal (E) skin surface representations. Statistical analysis was performed using ANOVA supplemented with multiple comparisons (contrast *post-hoc* tests). Horizontally aligned * and bars show statistical differences between the experimental groups. $P < 0.05$; **: $P < 0.01$; ***: $P < 0.001$; ****: $P < 0.0001$.

Figure 6

Schematically represented putative mechanisms illustrating the cortical effects of the unilateral vestibular neurectomy (UVN).

Left panel: *Main anatomical pathways conveying vestibular and somatosensory signals in intact animals (CTRL).* Vestibular nerves project ipsilaterally onto the vestibular nuclei (**VN**) which constitute the first relay of the vestibulo-spinal and vestibulo-thalamo-cortical pathways. Reciprocal commissural inhibition between VN is represented (-). Peripheral somatosensory afferents from the hindpaws that are conveyed via the lemniscal pathway form synapses in the gracile nucleus (**GN**). Second-order neurons cross the midline and project onto the contralateral thalamic nuclei (**Th**) in which the third-order neurons transmit somatosensory signals to the primary somatosensory cortex (**S1**).

Middle panel: *Immediate consequences of the UVN assessed during the first postlesion hours.* The vestibular deafferentation induces an imbalance between opposite VN, resulting from a hyperexcitability of the contralesional VN and a reduced activity of the ipsilesional one. This unilateral deafferentation leads to a syndrome characterized by vestibulo-ocular and postural asymmetries (not observed under anesthesia). Given the bilateral projections of vestibulo-thalamic inputs, with hypothetically dominant contralateral projections, presumably greater in the left hemisphere, the VN imbalance is expected to result in a decrease, however asymmetrical, of thalamo-cortical inputs in both S1 cortices. We postulate that the immediate expansion of cutaneous RFs reveals a reduction of net tonic inhibition normally exerted by vestibular projections onto S1 layer IV neurons, possibly via thalamo-cortical inputs and/or cortico-cortical connections. In normal

conditions, ongoing vestibular inhibitory influence may thus contribute to refining the size of S1 neurons' cutaneous RFs, i.e, to maintaining a fine somatotopic order in the cutaneous cortical maps, and consequently improve tactile spatial acuity on the foot sole during stance and locomotion, in order to optimize postural adjustments and body balance.

Right panel: *Consequences of the UVN at 35th days postlesion.* At this chronic stage of the vestibular compensation, a symmetry of excitability between VN is restored to a large extent. By contrast, our data indicate that the UVN rats displayed a strategy characterized by a shift of body weight distribution toward the ipsilesional hindpaw, presumably to increase somatosensory feedback for improving postural balance. We hypothesize that this increased body weight induced larger temporally co-stimulated ventral skin surfaces during posture and locomotion and therefore increased locally synchronized flow of tactilo-plantar inputs. Hence, consistently with the current knowledge on cortical plasticity mechanisms, this postural strategy would induce an experience-driven expansion of S1 neurons' cutaneous RFs located on the ipsilesional hindpaw.

S1: Primary somatosensory cortex
Th: Thalamus
GN: Gracile Nucleus
VN: Vestibular Nucleus
SC: Spinal Cord

Supplementary Figure 1

Effects of UVN on the ipsi- and contralesional hindpaw cortical maps obtained after double mapping.

Both ipsilesional and contralesional hindpaw representations were mapped in the same rat one hour (n=3) and 35 days (n=2) after UVN, starting with the hemisphere either ipsilateral or contralateral to the UVN. **A:** mean relative RF size (ventral, dorsal and ventral & dorsal) of intact (CTRL) and lesioned rats. Black dots represent individual RF size outlier values and boxplots represent first and third quartiles and medians. Red triangles show mean RF size. **B-C:** Separate mean relative RF size of ventral and dorsal skin RFs taken from the data shown in A. **D:** Mean mechanical threshold of neuronal responses obtained using Von Frey filaments (bending pressure). **E:** Mean size of hindpaw map area. **F:** Stacked histogram illustrating relative mean areas of the different subregions of the cortical maps normalized with respect to the hindlimb total surface area (green: *simple* regions; purple: *mixed* regions). **G-H:** Separate relative mean areas of the ventral and dorsal skin map territories taken from the data shown in F are also illustrated. Data of F to H are expressed as means ± SEM.

Figure 1

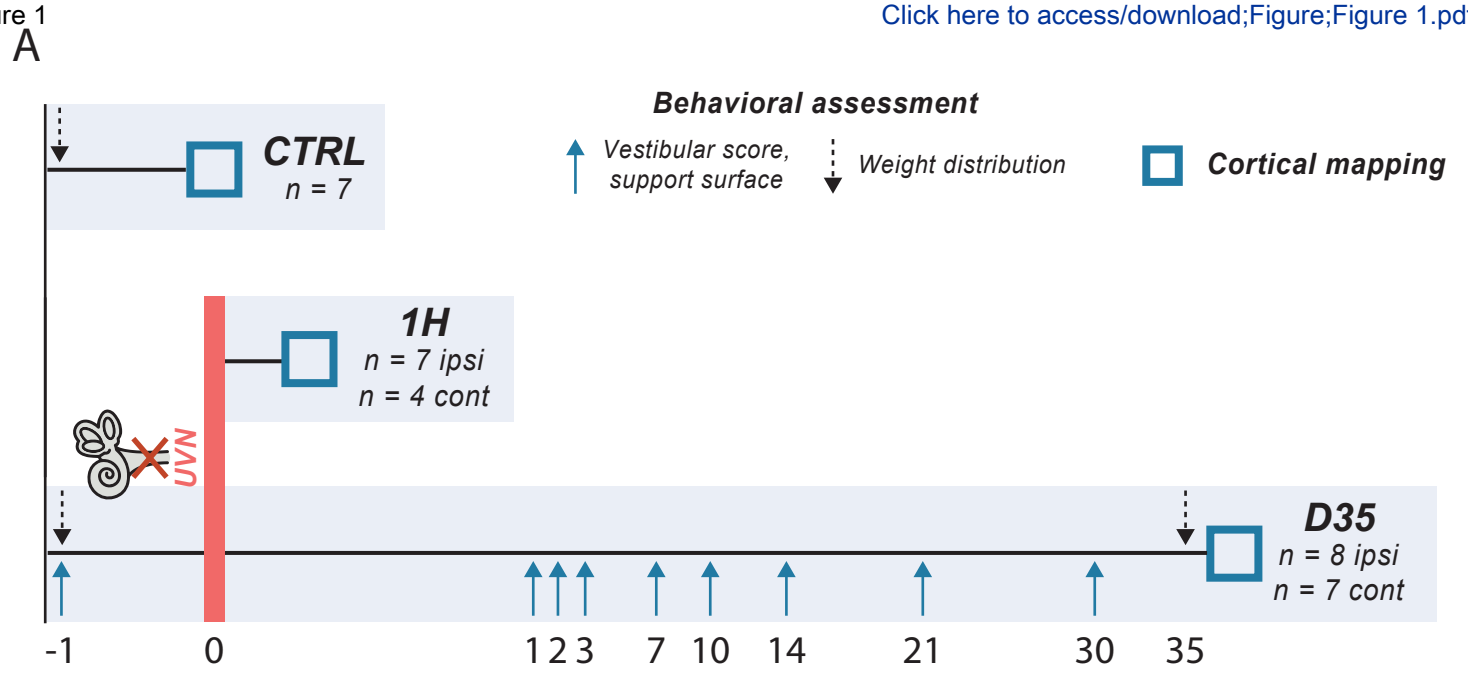

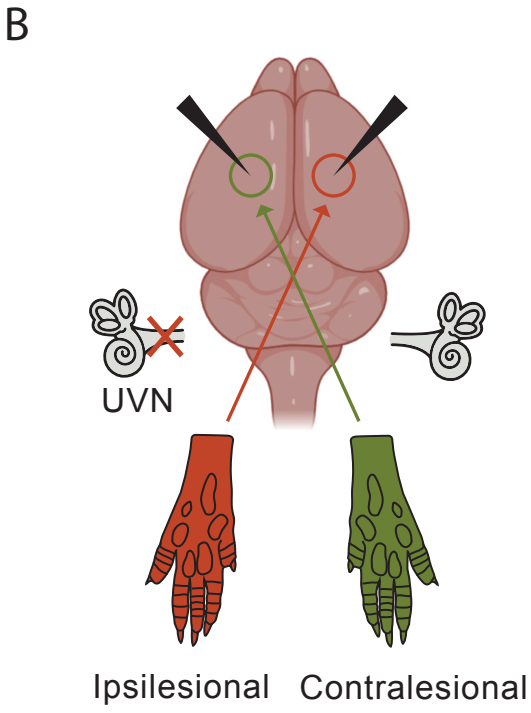

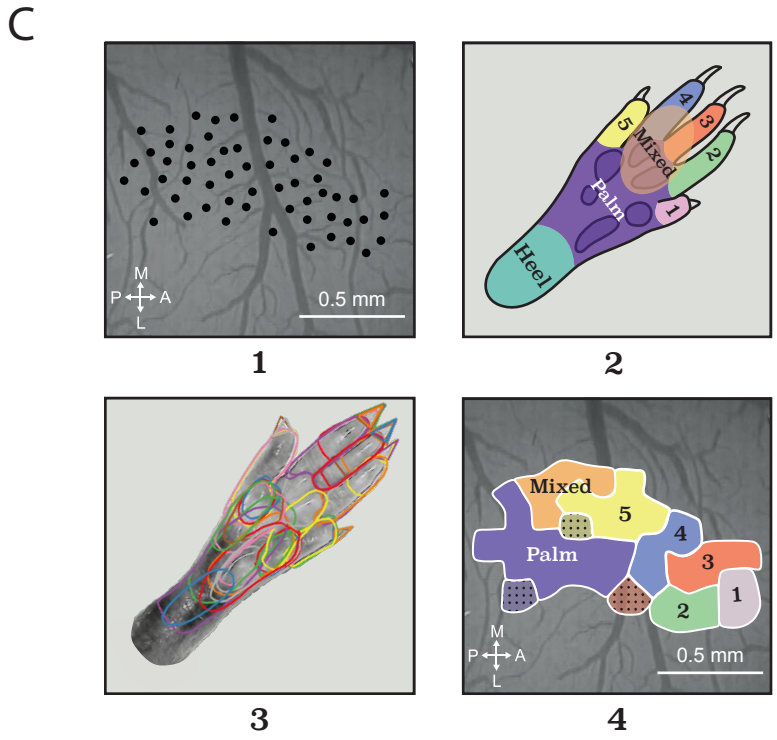

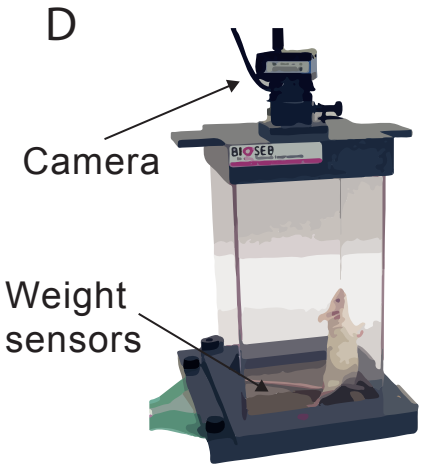

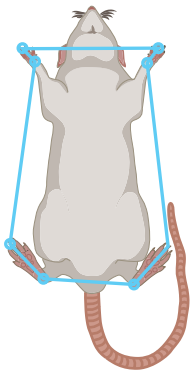

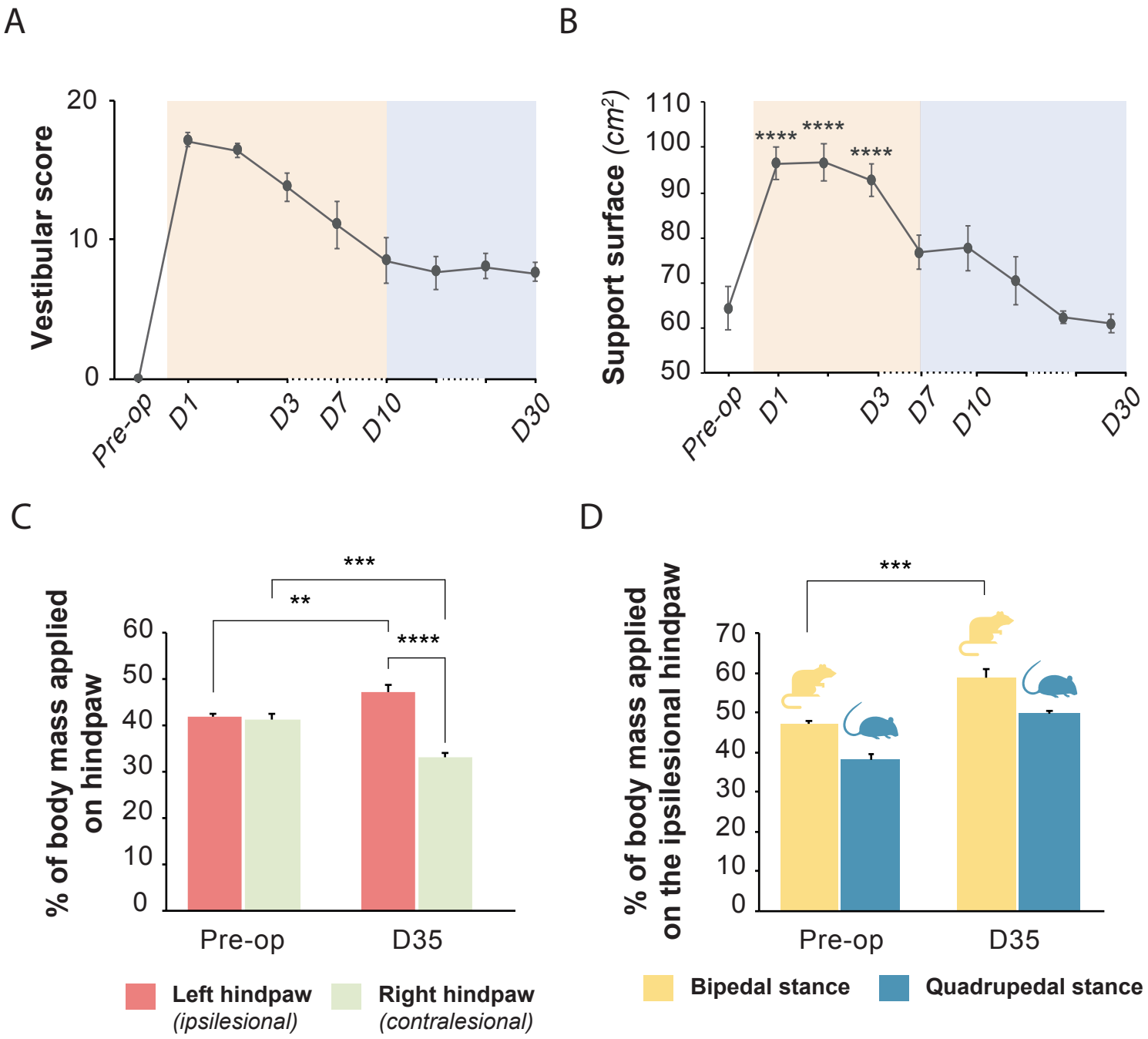

Figure 3

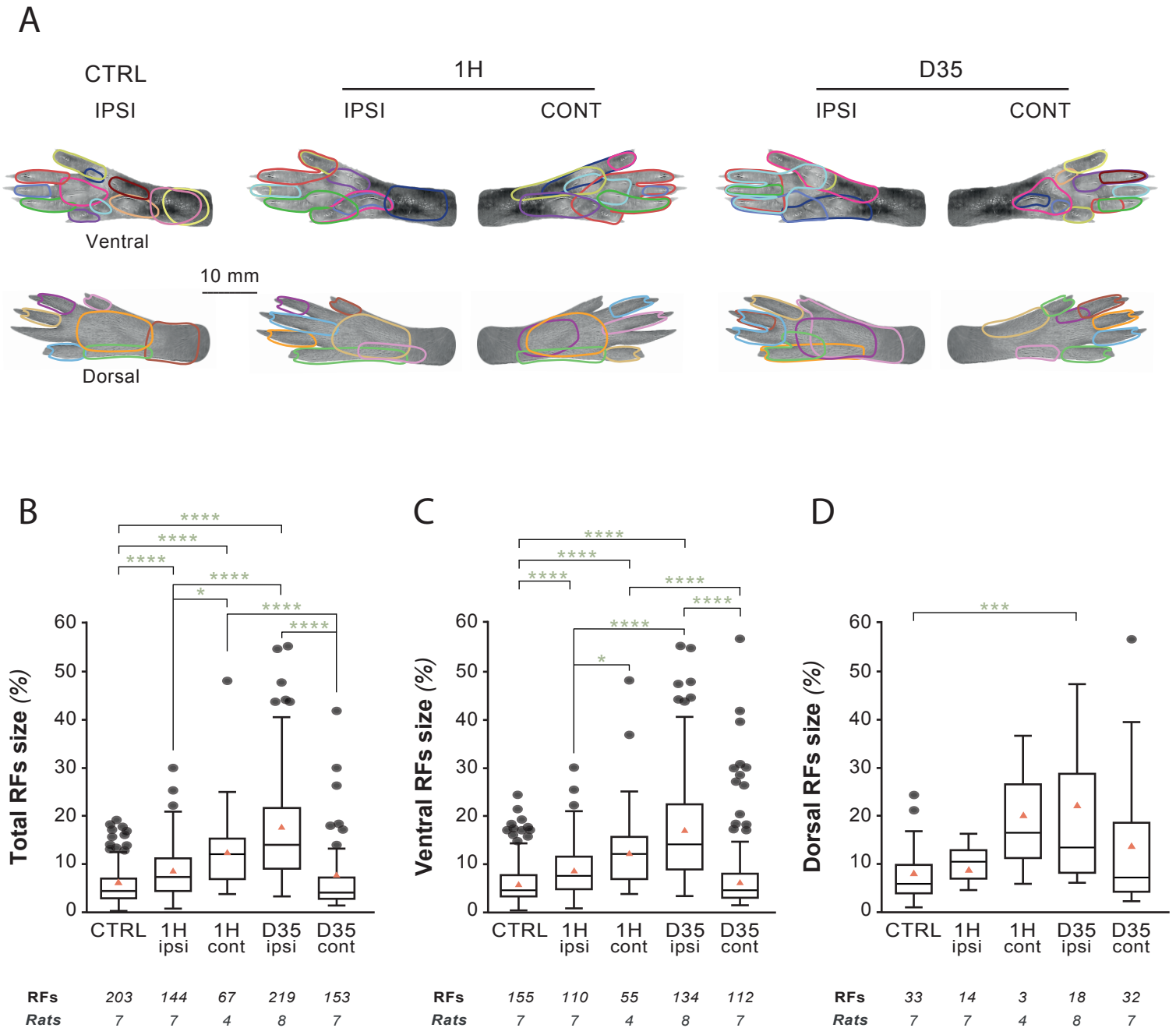

Figure 4

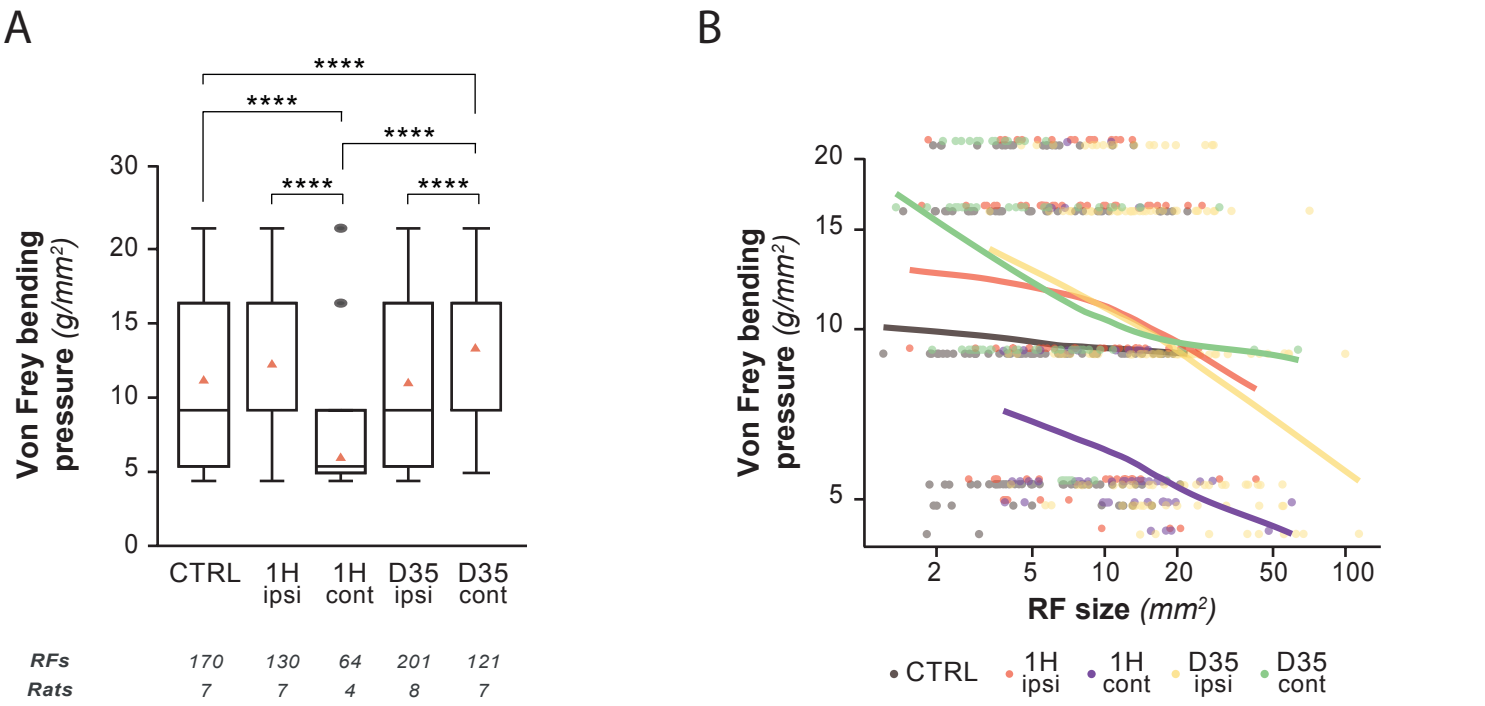

Figure 5

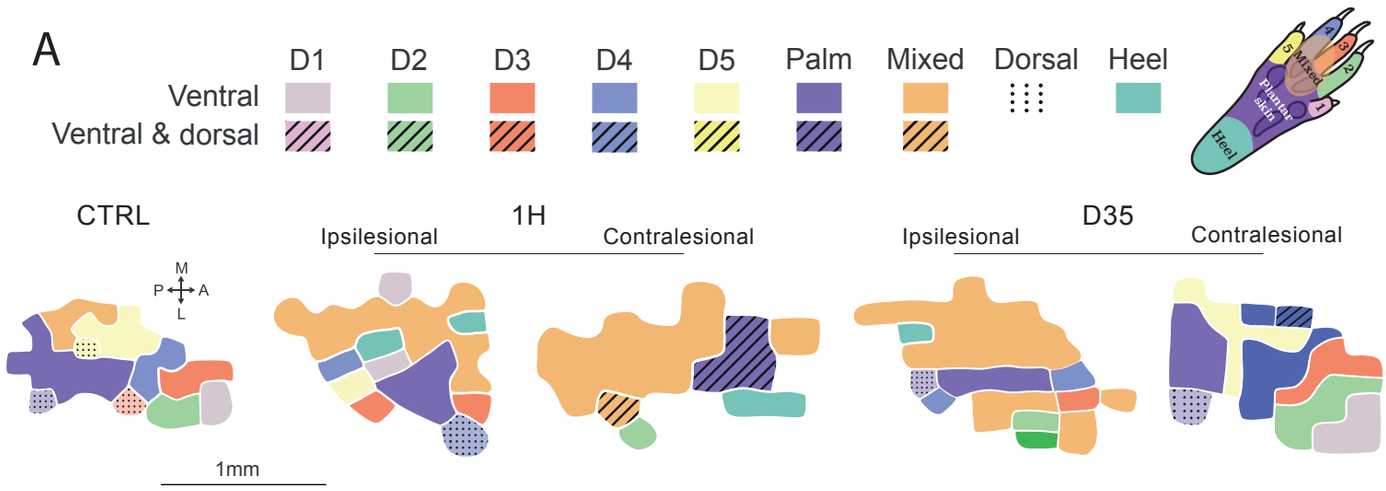

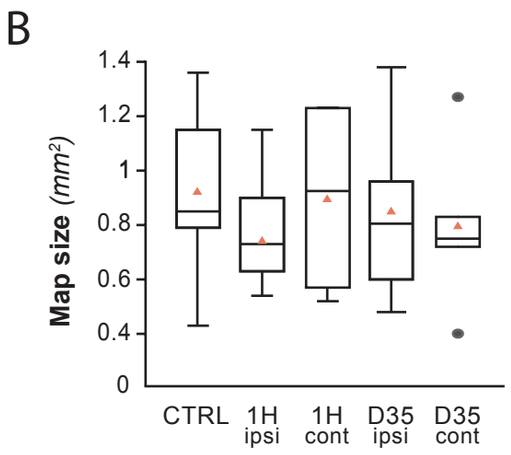

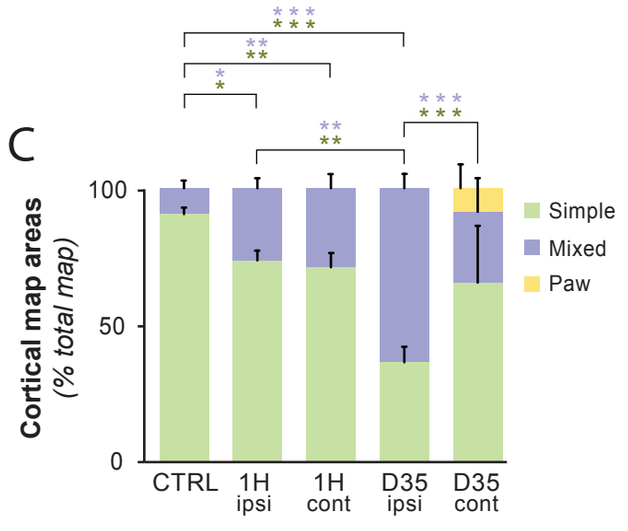

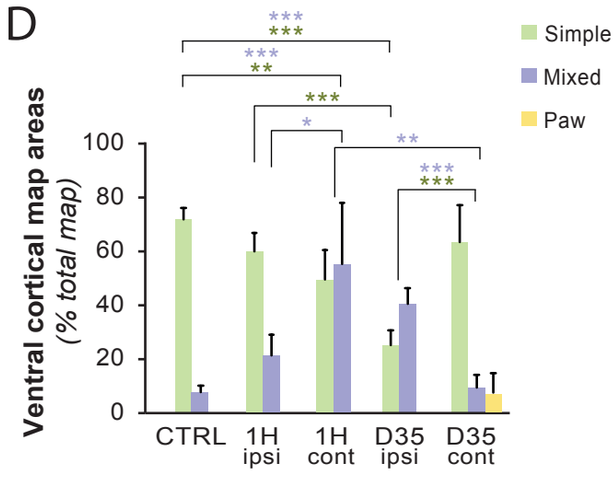

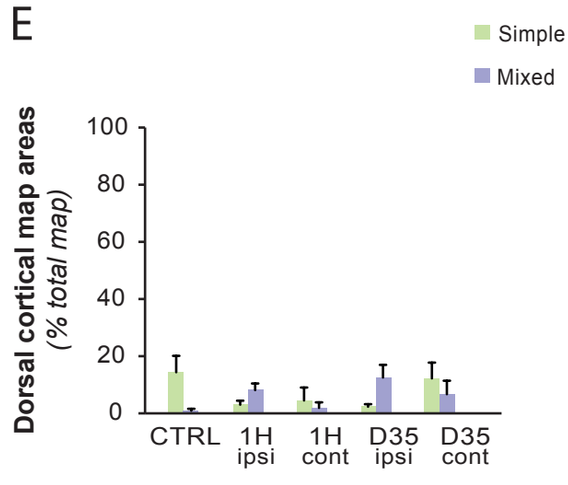

Figure 6